

A heteroclinic network in the $2 : \sqrt{3}$ mode interaction in Boussinesq convection

November 30, 2009

Sofia B.S.D. Castro

Centro de Matemática and Faculdade de Economia
Universidade do Porto
Rua Dr. Roberto Frias, 4200-464 Porto, Portugal
email: sdcastro@fep.up.pt

Isabel S. Labouriau

Centro de Matemática da Universidade do Porto
Rua do Campo Alegre 687, 4169-007 Porto, Portugal
email: islabour@fc.up.pt

Olga Podvigina

Observatoire de la Côte d'Azur, CNRS UMR 6529,
BP 4229, 06304 Nice Cedex 4, France
and International Institute of Earthquake Prediction Theory
and Mathematical Geophysics,
84/32 Profsoyuznaya St, 117997 Moscow, Russian Federation
email: olgap@ns3.mitp.ru

ABSTRACT.

We consider Boussinesq convection in a plane layer restricted to a hexagonal lattice, assuming that the trivial steady state becomes unstable to two modes of the form of rolls with spatial periods in the $2 : \sqrt{3}$ ratio. For the imposed periodicity, the symmetry group of the system is $\mathbf{D}_6 \times \mathbf{T}^2 \times \mathbf{Z}_2$. We analyse the restriction to a centre manifold parametrised by \mathbf{C}^6 and show that the normal form admits a complex heteroclinic network involving up to eight steady states of different symmetry types. In Boussinesq convection, due to relations between the normal form coefficients, only four types of steady states can be involved in the network. We examine the normal form restricted to \mathbf{R}^6 , a flow-invariant subspace, and describe the dynamics near the network that has switching at the nodes.

KEY WORDS AND PHRASES:

mode interaction, steady-state bifurcation, symmetry, robust heteroclinic network

CONTENTS

1. Introduction	3
2. Boussinesq convection in a plane layer	4
2.1. Equations	4
2.2. Symmetries	5
3. Definitions and preliminary results	5
4. Dynamics in \mathbf{C}^6	7
4.1. Normal form	7
4.2. Single-mode steady states in \mathbf{C}^3 . Heteroclinic connections.	7
4.3. Heteroclinic network in \mathbf{C}^6	9
5. Restriction to \mathbf{R}^6	10
5.1. Normal form	10
6. Network in \mathbf{R}^6	11
6.1. Quotient network	11
6.2. Motifs and cycles	13
6.3. Cycles in the network	14
7. Dynamics near the network	16
7.1. Switching at a node	16
7.2. Railroad switches	17
7.3. Stability of cycles	20
7.4. Discussion	21
References	22
Appendix A. Eigenspaces and eigenvalues near single-mode steady states	22

1. INTRODUCTION

Thermal convection, i.e., instability of fluid due to an imposed temperature gradient, has been extensively studied for more than a century, in particular, from the point of pattern formation and equivariant bifurcation theory. An interesting phenomenon, that has been detected in these investigations, is the existence of homoclinic and heteroclinic cycles.

The best known example of heteroclinic cycle is the Busse-Heikes cycle arising in Boussinesq convection in a rotating plane layer, when the rotation is sufficiently rapid. The cycle originates from the instability of rolls to perturbations of the form of rolls rotated by a finite angle with respect to the perturbed state (the Küppers-Lortz instability [15]). If the angle between the perturbed rolls and the perturbation is $2\pi/3$, a cycle connecting three roll flows is formed [7, 5]. Other types of instability can also result in the formation of heteroclinic cycles, for instance, emergence of smaller fundamental scales in the flow. Heteroclinic cycles related to the $1 : 2$ spatial resonance (i.e., emergence of a twice finer characteristic spatial scale) can emerge in the two-layer thermal convection [22] and in a single layer in a non-Boussinesq convection (see [21, 16] and references therein). In Rayleigh-Bénard convection with the midplane reflection symmetry the $1 : 3$ resonance plays an important role [17] (see, for instance, Porter and Knobloch [20]). A complex heteroclinic network in a normal form corresponding to the $1 : \sqrt{2}$ spatial resonance (the irrationality is due to the change of orientation of rolls, rotated by $\pi/4$) in Boussinesq convection was investigated by Podvigina and Ashwin [19].

In this paper we consider a heteroclinic network emerging in Boussinesq convection in a plane layer with an imposed hexagonal periodicity lattice, assuming that the trivial steady state of fluid at rest becomes unstable to two modes of the form of rolls with spatial periods in the $2 : \sqrt{3}$ ratio. The symmetry group of the system is $\mathbf{D}_6 \times \mathbf{T}^2 \times \mathbf{Z}_2$ and the centre eigenspace is \mathbf{C}^6 . We derive a general third-order ODE commuting with the action of the group on the centre eigenspace (a normal form of degree 3), with some fifth order terms included to resolve degeneracies. In each of the pure-mode subspaces, four symmetry types of steady state bifurcate when the trivial steady state becomes unstable. For this normal form we prove the existence of structurally stable heteroclinic connections which can form a heteroclinic network involving all eight types of primary steady states. In Boussinesq convection the network cannot involve more than four types of steady states because of inequalities satisfied by the normal form coefficients. However, the complete network can exist in another planar systems which has the same symmetry group.

Even with four types of steady states involved, the network is still difficult to study. Hence, we consider the system restricted to the flow-invariant subspace \mathbf{R}^6 and part of the network persisting there. We do not claim to have exhaustively studied all the features of the network but, given its complexity, settle for describing some of the interesting behaviour that may be observed in its vicinity. The dynamics near the heteroclinic network is determined by the existence of switching at nodes, by the stability of cycles in the network and by what we call *railroad switches*. The latter is a phenomenon that depends on the magnitude of some parameters. The existence of railroad switches means that, when two connections start at a node, trajectories near this node will follow one or the other of the connections, according to the relative magnitude of some parameters (two, in this case). Switching at a node guarantees the existence of trajectories near a node, from which two connections start, that follow both connections. The stability of a given cycle in the network makes it more easily observable in numerical simulations or experiments.

Our approach is one based on symmetry. We therefore make intensive use of the existence of flow-invariant spaces as a consequence of the symmetry. In fact, we study the dynamics near the heteroclinic network by restricting the equations to a 6-dimensional real flow-invariant vector space. This approach guarantees that the network and nearby dynamics persist for the original 12-dimensional real space. The connections that make up the network are also established by restriction to convenient invariant spaces, 2-dimensional this time. Symmetry is also used to describe the network itself in that we identify some motifs which, when iterated by symmetry, will produce the whole network. Finally, we show that under some conditions one of the cycles in the network is essentially asymptotically stable and for this symmetry is extensively used, again.

The text proceeds as follows: in the next section, we describe Boussinesq convection in a plane layer, introducing the symmetries of the problem as well as a normal form, its steady states and stability which are relevant for our work. Then, after some preliminary results in Section 3, we obtain normal forms for the dynamics in the 12-dimensional centre manifold (parametrised by \mathbf{C}^6) for the two-mode problem

and discuss some previous results on a single mode (the restriction to \mathbf{C}^3). Section 6 is devoted to the description of the heteroclinic network in the restriction to a flow-invariant submanifold of dimension 6 (parametrised by \mathbf{R}^6). We prove the existence of all connections, and describe the network using the notions of cycles and motifs and we present the results of numerical simulations that illustrate well the behaviour along the network. In section 7 we study the dynamics near the network. We address the issue of switching at a node of the network and prove the existence of switching at the two types of nodes: rolls and pathwork quilts. We show that although there is switching, at some nodes there is a connection that is preferred by nearby trajectories. We also look at the stability of cycles in the network. The appendix contains the technical information concerning eigenvalues and eigenspaces near single-mode steady states.

2. BOUSSINESQ CONVECTION IN A PLANE LAYER

2.1. Equations. Consider the non-dimensional equations for Boussinesq convection in a plane layer $0 < z < 1$ uniformly heated from below. The flow \mathbf{v} and pressure p satisfy the Navier-Stokes equation

$$(1) \quad \frac{\partial \mathbf{v}}{\partial t} = \mathbf{v} \times (\nabla \times \mathbf{v}) + P \Delta \mathbf{v} + PR \theta \mathbf{e}_z - \nabla p$$

and the incompressibility condition

$$(2) \quad \nabla \cdot \mathbf{v} = 0.$$

The heat transfer equation

$$(3) \quad \frac{\partial \theta}{\partial t} = -(\mathbf{v} \cdot \nabla) \theta + v_z + \Delta \theta$$

determines the evolution of θ , the difference between the temperature in the flow and the linear temperature profile. The parameters R and P are the Rayleigh and Prandtl numbers, respectively. We assume stress-free boundary conditions for the flow and fixed temperature on horizontal boundaries:

$$(4) \quad \frac{\partial v_x}{\partial z} = \frac{\partial v_y}{\partial z} = v_z = 0, \quad \theta = 0 \quad \text{at } z = 0, 1.$$

Flows defined in a hexagonal cell are invariant under translations by

$$(5) \quad \mathbf{e}_1 = L(1, 0), \quad \mathbf{e}_2 = L\left(\frac{1}{2}, \frac{\sqrt{3}}{2}\right)$$

in the (x, y) -plane (see [10]), i.e.

$$(6) \quad \mathbf{v}(x, y, z) = \mathbf{v}((x, y) + p\mathbf{e}_1 + q\mathbf{e}_2, z) \text{ and } \theta(x, y, z) = \theta((x, y) + p\mathbf{e}_1 + q\mathbf{e}_2, z)$$

for any $(p, q) \in \mathbf{Z}^2$.

The system Eq. (1)-Eq. (4) admits the trivial solution $\mathbf{v} = 0$, $\theta = 0$ describing pure thermal conduction. The steady state becomes unstable to perturbations with a wavenumber k at $R = (k^2 + \pi^2)^3 k^{-2}$; the perturbation mode is

$$(7) \quad \mathbf{V}(k) = \begin{pmatrix} -\pi k^{-1} \cos \pi z \sin kx \\ 0 \\ \sin \pi z \cos kx \\ (k^2 + \pi^2)^{-1} \sin \pi z \cos kx \end{pmatrix}.$$

(More eigenmodes are obtained by application of symmetries of the system.) The critical Rayleigh number for the onset of convection is $R = \frac{27}{4} \pi^4 \approx 657.5$, and the critical wavenumber is $k_c = \pi/\sqrt{2}$.

Modes with wave numbers k and $2k/\sqrt{3}$ become unstable simultaneously at $R_m = \pi^4 2^{-4/3} 3^{-2/3} (2^{4/3} - 3^{2/3})^{-2} (2^{2/3} - 3^{1/3})^{-1} \approx 662.1$, the critical wavenumber is $k_m = \pi 3^{1/3} 2^{-1/3} (2^{2/3} + 3^{1/3})^{-1/2} \approx 2.07$. Consider the mode with the wavenumber $2k/\sqrt{3}$

$$(8) \quad \mathbf{W}(k) = \begin{pmatrix} 0 \\ -\pi (2k/\sqrt{3})^{-1} \cos \pi z \sin 2k/\sqrt{3}y \\ \sin \pi z \cos 2k/\sqrt{3}y \\ (4k^2/3 + \pi^2)^{-1} \sin \pi z \cos 2k/\sqrt{3}y \end{pmatrix}.$$

The modes (7) and (8) are both periodic on the hexagonal lattice (5) with $L = 4\pi k_m^{-1}$.

2.2. Symmetries. The symmetry group of the convective system Eq. (1)-Eq. (3) with the boundary conditions Eq. (4,6) is $\Gamma = \mathbf{D}_6 \times \mathbf{T}^2 \times \mathbf{Z}_2$. The group \mathbf{D}_6 is the 12-element group of symmetries of the hexagonal cell, including the cyclic group of rotations generated by

$$\rho : (x, y, z) \mapsto \left(\frac{1}{2}x + \frac{\sqrt{3}}{2}y, \frac{\sqrt{3}}{2}x - \frac{1}{2}y, z\right),$$

and reflections, in particular,

$$\begin{aligned} s_1 : (x, y, z) &\mapsto (x, -y, z), \\ s_2 : (x, y, z) &\mapsto (-x, y, z), \\ s_3 : (x, y, z) &\mapsto (-x, -y, z). \end{aligned}$$

The groups \mathbf{T}_1 and \mathbf{T}_2 are the groups of translations by along the e_1 and e_2 directions, respectively:

$$\gamma_\alpha^1 : (x, y, z) \mapsto (x + \alpha L(2\pi)^{-1}, y, z)$$

and

$$\gamma_\alpha^2 : (x, y, z) \mapsto \left(x - \frac{1}{2}\alpha L(2\pi)^{-1}, y + \frac{\sqrt{3}}{2}\alpha L(2\pi)^{-1}, z\right)$$

where $0 \leq \alpha < 2\pi$ (so that $\gamma_{\frac{1}{2}\pi}^1 = \gamma_{\frac{1}{2}\pi}^2 = e$). The group \mathbf{Z}_2 is generated by the so-called Boussinesq symmetry, which is a reflection about the horizontal midplane:

$$r : (x, y, z) \mapsto (x, y, 1 - z).$$

Consider the centre eigenspace spanned by rolls, Eq. (7,8), and their symmetric images

$$(9) \quad \begin{aligned} \mathbf{X}_1 = \mathbf{V}, \quad \mathbf{Y}_1 = \gamma_{\pi/2}^2 \mathbf{V}, \quad \mathbf{X}_{2,3} = \rho^{2,4} \mathbf{V}, \quad \mathbf{Y}_{2,3} = \rho^{2,4} \mathbf{Y}_1, \\ \mathbf{X}_4 = \mathbf{W}, \quad \mathbf{Y}_4 = \gamma_{\pi/4}^2 \mathbf{W}, \quad \mathbf{X}_{5,6} = \rho^{2,4} \mathbf{W} \text{ and } \mathbf{Y}_{5,6} = \rho^{2,4} \mathbf{Y}_4. \end{aligned}$$

We identify this 12-dimensional subspace to \mathbf{C}^6 and use these coordinates to parametrise the centre manifold. The coordinates $(z_1, z_2, z_3, w_1, w_2, w_3) \in \mathbf{C}^6$ on the centre manifold, that we introduce, are projections in the directions \mathbf{X}_j and \mathbf{Y}_j for z_j and \mathbf{X}_{j+3} and \mathbf{Y}_{j+3} for w_j , $j = 1, 2, 3$.

The symmetries of the system transform the coordinates in the following way:

$$\begin{aligned} \rho : (\mathbf{z}, \mathbf{w}) &\mapsto (\bar{z}_2, \bar{z}_3, \bar{z}_1, \bar{w}_2, \bar{w}_3, \bar{w}_1), \\ \rho^2 : (\mathbf{z}, \mathbf{w}) &\mapsto (z_3, z_1, z_2, w_3, w_1, w_2), \\ s_1 : (\mathbf{z}, \mathbf{w}) &\mapsto (z_1, z_3, z_2, \bar{w}_1, \bar{w}_3, \bar{w}_2), \\ s_2 : (\mathbf{z}, \mathbf{w}) &\mapsto (\bar{z}_1, \bar{z}_3, \bar{z}_2, w_1, w_3, w_2), \\ s_3 : (\mathbf{z}, \mathbf{w}) &\mapsto (\bar{z}_1, \bar{z}_2, \bar{z}_3, \bar{w}_1, \bar{w}_2, \bar{w}_3), \\ \gamma_\alpha^1 : (\mathbf{z}, \mathbf{w}) &\mapsto (e^{2i\alpha} z_1, e^{-i\alpha} z_2, e^{-i\alpha} z_3, w_1, e^{-2i\alpha} w_2, e^{2i\alpha} w_3), \\ \gamma_\alpha^2 : (\mathbf{z}, \mathbf{w}) &\mapsto (e^{i\alpha} z_1, e^{i\alpha} z_2, e^{-2i\alpha} z_3, e^{2i\alpha} w_1, e^{-2i\alpha} w_2, w_3), \\ \gamma_\alpha^3 = \gamma_\alpha^1 \gamma_{-2\alpha}^2 : (\mathbf{z}, \mathbf{w}) &\mapsto (z_1, e^{-3i\alpha} z_2, e^{3i\alpha} z_3, e^{-4i\alpha} w_1, e^{2i\alpha} w_2, e^{2i\alpha} w_3), \\ r : (\mathbf{z}, \mathbf{w}) &\mapsto (-\mathbf{z}, -\mathbf{w}). \end{aligned}$$

From now on we study the restriction to the centre manifold, where the system reduces to an ordinary differential equation with these symmetries in 12 dimensions.

3. DEFINITIONS AND PRELIMINARY RESULTS

Let f be a smooth vector field in \mathbf{R}^n . Given two equilibrium points A and B of $\dot{x} = f(x)$, a *heteroclinic connection* from A to B , denoted $A \rightarrow B$, is a trajectory contained in the unstable manifold $W^u(A)$ of A and in the stable manifold $W^s(B)$ of B . A *heteroclinic cycle* is a finite ordered set of equilibria $\{A_j : j = 1, \dots, k\}$ together with connections $A_j \rightarrow A_{j+1}$ with $A_{k+1} = A_1$. We refer to the equilibria defining the heteroclinic cycle as *nodes*. A *heteroclinic network* is a connected set that is a finite union of heteroclinic cycles.

A heteroclinic connection $A \rightarrow B$ where $W^u(A)$ and $W^s(B)$ are not transverse may be easily broken by an arbitrarily small perturbation of the vector field. A simple calculation of dimensions shows that it is not possible to have a heteroclinic cycle in \mathbf{R}^n with all connections arising at transverse intersections.

Thus, for general vector fields, heteroclinic cycles are not a robust feature. The situation changes when there is some underlying symmetry, as we proceed to discuss.

Let G be a compact Lie group acting linearly on \mathbf{R}^n . The vector field f is G -equivariant if for all $\gamma \in G$ and $x \in \mathbf{R}^n$, we have $f(\gamma x) = \gamma f(x)$. In this case $\gamma \in G$ is said to be a symmetry of f . We refer the reader to Golubitsky, Stewart and Schaeffer [10] for more information on differential equations with symmetry.

The G -orbit of $A \in \mathbf{R}^n$ is the set $[A] = \{\gamma A, \gamma \in G\}$ that is invariant under the flow of G -equivariant vector fields f . In particular, if A and B are equilibria of $\dot{x} = f(x)$, so are the elements in their G -orbits and if there is a trajectory $\varphi(t)$ making a connection $A \rightarrow B$, then for $\gamma \in G$ the trajectory $\gamma\varphi(t)$ is a connection $\gamma A \rightarrow \gamma B$. We refer to this G -orbit of connections as a *quotient connection* and we indicate this with the notation $[A] \rightarrow [B]$. The reader should be warned that this does *not* mean there is a connection $\gamma A \rightarrow \delta B$ for any $\gamma, \delta \in G$ even though $\gamma A \in [A]$, $\delta B \in [B]$. We use a similar notation for *quotient cycle* and *quotient network*.

The *isotropy subgroup* of $x \in \mathbf{R}^n$ is $G_x = \{\gamma \in G, \gamma x = x\}$. For an isotropy subgroup S of G , its *fixed-point subspace* is

$$\text{Fix}(S) = \{x \in \mathbf{R}^n : \forall \gamma \in S, \gamma x = x\}.$$

If f is G -equivariant then $\text{Fix}(S)$ is flow-invariant.

For a differential equation in a plane with two equilibria A and B , if A is a saddle and B is a sink then a connection $A \rightarrow B$ is a transverse intersection of $W^u(A)$ and $W^s(B)$ and thus persists under small perturbations of the equations. If f is G -equivariant and the plane is the fixed-point subspace of an isotropy subgroup of G , then both the flow-invariance of the plane and the existence of the connection persist under small perturbations that preserve the symmetry. This is the reason for the robustness of heteroclinic cycles and networks in symmetric dynamics.

To prove the existence of heteroclinic connections in invariant planes we use a theorem from [18]. For completeness of the presentation the statement of the theorem is given below.

Consider a system of the form

$$(10) \quad \begin{aligned} \dot{x} &= (\lambda + b_1 x^2 + b_2 y^2)x, \\ \dot{y} &= (\mu + c_1 y^2 + c_2 x^2)y, \end{aligned}$$

assuming

$$(11) \quad \lambda > 0, \mu > 0, b_1 < 0, c_1 < 0.$$

then for arbitrary b_2 and c_2 there exist steady states $S_1 = (x_1, 0) = (\pm\sqrt{-\lambda/b_1}, 0)$ and $S_2 = (0, y_2) = (0, \pm\sqrt{-\mu/c_1})$, which are stable along the directions $(x, 0)$ and $(0, y)$, respectively.

Theorem 3.1 (Podvigina,[18]). *The system (10),(11) can exhibit the following four generic types of behavior:*

(i). *If $\lambda - \frac{\mu b_2}{c_1} < 0$, $\mu - \frac{\lambda c_2}{b_1} < 0$, then the steady states S_1 and S_2 are stable, there exist an unstable steady state $S_3 = (x_3, y_3)$, $x_3 y_3 \neq 0$, and heteroclinic connections from S_3 to S_1 and S_2 .*

(ii). *If $\lambda - \frac{\mu b_2}{c_1} < 0$, $\mu - \frac{\lambda c_2}{b_1} > 0$, then the only steady states of the system are $S_0 = (0, 0)$, S_1 and S_2 , S_1 is unstable and S_2 is stable, and there exists a heteroclinic connection from S_1 to S_2 .*

(ii'). *If $\lambda - \frac{\mu b_2}{c_1} > 0$, $\mu - \frac{\lambda c_2}{b_1} < 0$, then the only steady states of the system are $S_0 = (0, 0)$, S_1 and S_2 , S_1 is stable and S_2 is unstable, and there exists a heteroclinic connection from S_2 to S_1 .*

(iii). *If $\lambda - \frac{\mu b_2}{c_1} > 0$, $\mu - \frac{\lambda c_2}{b_1} > 0$, $b_1 c_1 - b_2 c_2 > 0$, then the steady states S_1 and S_2 are unstable, there exist a stable steady state $S_3 = (x_3, y_3)$, $x_3 y_3 \neq 0$, and heteroclinic connections from S_1 and S_2 to S_3 .*

(iv). *If $\lambda - \frac{\mu b_2}{c_1} > 0$, $\mu - \frac{\lambda c_2}{b_1} > 0$, $b_1 c_1 - b_2 c_2 < 0$, then the only steady states of the system are $S_0 = (0, 0)$, S_1 and S_2 , all the three are unstable. Any trajectory $(x(x_0, y_0, t), y(x_0, y_0, t))$ starting at any point (x_0, y_0) , $x_0 y_0 \neq 0$, escapes to infinity, i.e. $\lim_{t \rightarrow \infty} x(x_0, y_0, t) = \infty$, $\lim_{t \rightarrow \infty} y(x_0, y_0, t) = \infty$.*

4. DYNAMICS IN \mathbf{C}^6

4.1. Normal form. The normal form on \mathbf{C}^6 for the considered action of the symmetry group $\Gamma = \mathbf{D}_6 \times \mathbf{T}^2 \times \mathbf{Z}_2$ truncated at cubic order (with one fifth-order term determining relative stability of triangles and hexagons included) is:

$$(12) \quad \begin{aligned} \dot{z}_1 &= \lambda_1 z_1 + z_1 [A_1 |z_1|^2 + A_2 (|z_2|^2 + |z_3|^2) + C_1 |w_1|^2 + C_2 (|w_2|^2 + |w_3|^2)] + \\ &\quad + A_3 \bar{z}_1 \bar{z}_2^2 \bar{z}_3^2 + C_3 \bar{z}_1 \bar{w}_2 w_3, \\ \dot{w}_1 &= \lambda_2 w_1 + w_1 [B_1 |w_1|^2 + B_2 (|w_2|^2 + |w_3|^2) + C_4 |z_1|^2 + C_5 (|z_2|^2 + |z_3|^2)] + \\ &\quad + B_3 \bar{w}_1 \bar{w}_2^2 \bar{w}_3^2 + C_6 (w_2 \bar{z}_3^2 + w_3 \bar{z}_2^2), \end{aligned}$$

where A_i , B_i and C_i are real numbers (the normal form coefficients). The equations for \dot{z}_j and \dot{w}_j , $j = 2, 3$, are obtained by applying the symmetry ρ^2 .

4.2. Single-mode steady states in \mathbf{C}^3 . Heteroclinic connections. In this section we highlight some of the patterns, and heteroclinic connections among them, occurring in single-mode in a system with $\mathbf{D}_6 \times \mathbf{T}^2 \times \mathbf{Z}_2$ -symmetry in \mathbf{C}^3 . These will persist when a second mode is introduced and become part of a heteroclinic network with connections between different modes. The subspaces $(\mathbf{z}; \mathbf{0})$ and $(\mathbf{0}; \mathbf{w})$ are invariant, because they are fixed-point subspaces for the groups \mathbf{Z}_3 (generated by $\gamma_{2\pi/3}^3$) and \mathbf{D}_2 (generated by γ_π^1 and γ_π^2), respectively. The system (12) restricted to $(\mathbf{z}; \mathbf{0})$ or $(\mathbf{0}; \mathbf{w})$ has the form

$$(13) \quad \begin{aligned} \dot{z}_1 &= \lambda z_1 + z_1 (a_1 |z_1|^2 + a_2 (|z_2|^2 + |z_3|^2)) + a_3 \bar{z}_1 \bar{z}_2^2 \bar{z}_3^2, \\ \dot{z}_2 &= \lambda z_2 + z_2 (a_1 |z_2|^2 + a_2 (|z_1|^2 + |z_3|^2)) + a_3 \bar{z}_2 \bar{z}_1^2 \bar{z}_3^2, \\ \dot{z}_3 &= \lambda z_3 + z_3 (a_1 |z_3|^2 + a_2 (|z_1|^2 + |z_2|^2)) + a_3 \bar{z}_3 \bar{z}_1^2 \bar{z}_2^2. \end{aligned}$$

Bifurcations in the system (13) with the action of $\mathbf{D}_6 \times \mathbf{T}^2 \times \mathbf{Z}_2$ generated by

$$\begin{aligned} \tilde{\rho} : (\mathbf{z}) &\mapsto (\bar{z}_2, \bar{z}_3, \bar{z}_1), \\ \tilde{s}_1 : (\mathbf{z}) &\mapsto (z_1, z_3, z_2), \\ \tilde{\gamma}_\alpha^1 : (\mathbf{z}) &\mapsto (e^{i\alpha} z_1, e^{-i\alpha} z_2, z_3), \\ \tilde{\gamma}_\alpha^2 : (\mathbf{z}) &\mapsto (z_1, e^{-i\alpha} z_2, e^{i\alpha} z_3), \\ \tilde{r} : (\mathbf{z}, \mathbf{w}) &\mapsto (-\mathbf{z}, -\mathbf{w}). \end{aligned}$$

were studied in [11], in particular, four types of steady states bifurcating at $\lambda = 0$ were found (see Table 1). One type of steady state is stable if all four bifurcate supercritically, which takes place if

$$(14) \quad a_1 < 0 \text{ and } a_1 + 2a_2 < 0.$$

Rolls (R) are stable if $a_1 - a_2 > 0$, hexagons (H) if $a_1 - a_2 < 0$ and $a_3 > 0$ and triangles (RT) if $a_1 - a_2 < 0$ and $a_3 < 0$. Note that the sign of a_3 can be reversed by the change of variables $\mathbf{z} \mapsto i\mathbf{z}$. Patchwork quilts (PQ) are always unstable.

If all branches bifurcate supercritically, the system (13) admits heteroclinic connection, which is proven in the following theorem. Some of the connections are displayed in Figure 1.

Theorem 4.1. *Consider the system (13), (14) where*

$$(15) \quad 0 < \lambda < \max \left(\left| \frac{(a_1 + 2a_2)^2}{4a_3} \right|, \left| \frac{2a_1 a_2}{a_3} \right|, \left| \frac{a_1^2 - a_2^2}{a_3} \right| \right).$$

then:

(i). If

$$(16) \quad a_1 - a_2 > 0,$$

the following heteroclinic connections exist: $PQ \rightarrow R$, $RT \rightarrow R$, $H \rightarrow R$, $H \rightarrow PQ$ and $RT \rightarrow PQ$.

(ii). If

$$(17) \quad a_1 - a_2 < 0,$$

the following connections exist: $R \rightarrow PQ$, $R \rightarrow RT$, $R \rightarrow H$, $PQ \rightarrow H$ and $PQ \rightarrow RT$.

Proof. (i) Consider the system (13) restricted to the subspace $(x_1, x_2, 0)$ which is invariant, because it is a fixed point subspace for the group \mathbf{D}_2 generated by $\tilde{\rho}^3$ and $\tilde{r}\tilde{\gamma}_\pi^1$. The conditions (14) and (15) imply existence of PQ= $(x_1 = x_{PQ}, x_2 = x_{PQ})$ and R= $(x_1 = x_R, 0)$, (16) implies stability of R and $\rho R = (0, x_R)$. Therefore, by Theorem 3.1 there exist heteroclinic connections from PQ to R and ρR .

Assume $a_3 > 0$. If (15) is satisfied, there exist two types of hexagons (x_H^+, x_H^+, x_H^+) and (x_H^-, x_H^-, x_H^-) where

$$x_H^\pm = \frac{-(a_1 + 2a_2) \pm ((a_1 + 2a_2)^2 - 4\lambda a_3)^{1/2}}{2a_3},$$

(x_H^-, x_H^-, x_H^-) bifurcates from $\mathbf{0}$ when λ becomes positive. There exists one type of triangles (ix_T, ix_T, ix_T) with

$$x_T = \frac{(a_1 + 2a_2) + ((a_1 + 2a_2)^2 + 4\lambda a_3)^{1/2}}{2a_3}.$$

Consider the system (13) restricted to the subspaces (x_1, x_2, x_2) , which is a fixed point subspace for the group \mathbf{D}_2 generated by $\tilde{\rho}^3$ and \tilde{s}_1

$$(18) \quad \begin{aligned} \dot{x}_1 &= \lambda x_1 + x_1(a_1 x_1^2 + 2a_2 x_2^2) + a_3 x_1 x_2^4, \\ \dot{x}_2 &= \lambda x_2 + x_2(a_1 x_2^2 + a_2(x_1^2 + x_2^2)) + a_3 x_2^3 x_1^2. \end{aligned}$$

Theorem 3.1 is not applicable to the system, because it contains fifth order terms. The condition (15) implies that any steady state in the subspace satisfied either $x_1 x_2 = 0$ or $x_1 = x_2$. The steady states R= $(x_R, 0)$ and PQ= $(0, x_{PQ})$ are stable, the steady state H= (x_H^-, x_H^-, x_H^-) is unstable in the $(q, -q)$ direction (see Table 1). Consider the triangle bounded by the lines $x_1 = 0$, $x_1 = x_2$ and $x_2 = \tilde{x}_2$, where $x_{PQ} < \tilde{x}_2 < x_H^+$. (15) implies that $x_{PQ} < x_H^+$. The lines $x_1 = 0$ and $x_1 = x_2$ are invariant subspaces of (13), \dot{x}_2 is negative in the interval $(x_2 = \tilde{x}_2, 0 \leq x_1 \leq \tilde{x}_2)$ because it is negative at both endpoints of the interval. Therefore, no trajectories escape from the triangle and hence the unstable manifold of H approaches PQ. Existence of connection from H to R is proven by considering the triangle bounded by the lines $x_2 = 0$, $x_1 = x_2$ and $x_1 = \tilde{x}_1$, where $x_R < \tilde{x}_1 < x_H^+$.

The subspace (ix_1, ix_2, ix_2) is a fixed point subspace for the group \mathbf{D}_2 generated by $\tilde{r}\tilde{\rho}^3$ and \tilde{s}_1 , the restriction of (13) to the subspace is

$$(19) \quad \begin{aligned} \dot{x}_1 &= \lambda x_1 + x_1(a_1 x_1^2 + 2a_2 x_2^2) - a_3 x_1 x_2^4, \\ \dot{x}_2 &= \lambda x_2 + x_2(a_1 x_2^2 + a_2(x_1^2 + x_2^2)) - a_3 x_2^3 x_1^2. \end{aligned}$$

The steady states R= $(ix_R, 0)$ and PQ= $(0, ix_{PQ})$ are stable, T= (ix_T, ix_T, ix_T) is unstable in the $(q, -q)$ direction. Similarly to above, trajectories are trapped in the triangle bounded by $x_1 = 0$, $x_1 = x_2$ and $x_2 = \tilde{x}_2$, where $\tilde{x}_2 > x_{PQ}$ and hence there exists a heteroclinic connection from T to PQ. Existence of the connection T→R is proven because trajectories are trapped in the triangle $x_2 = 0$, $x_1 = x_2$ and $x_1 = \tilde{x}_1$, where $\tilde{x}_1 > x_R$.

The case $a_3 < 0$ is treated similarly to the case $a_3 > 0$. For the case (ii) the proof is identical to the case (i). \square

Note that near the bifurcation point λ is small and therefore (15) is satisfied.

The dynamics in $(x + iy, x + iy, x + iy)$ is more complex, compared to the 2-dimensional subspaces considered in Theorem 4.1. The subspace $(x + iy, x + iy, x + iy)$ is a fixed point subspace for the group \mathbf{Z}_3 generated by $\tilde{\rho}^2$. The system (13) restricted onto this subspace is

$$(20) \quad \begin{aligned} \dot{x} &= \lambda x + x(a_1 + 2a_2)(x^2 + y^2) + a_3 x(x^4 + 5y^4 - 10x^2 y^2), \\ \dot{y} &= \lambda y + y(a_1 + 2a_2)(x^2 + y^2) - a_3 y(y^4 + 5x^4 - 10x^2 y^2). \end{aligned}$$

Assume $a_3 > 0$ (the case $a_3 < 0$ is identical).

In addition to the steady states $x = x_H^\pm$ and $y = x_T$, the system admits steady states (x_u^\pm, y_u^\pm) , where $3(x_u^\pm)^2 = (y_u^\pm)^2$, $(x_u^\pm)^2 + (y_u^\pm)^2 = (x_H^\pm)^2$ and (x_l, y_l) , where $x_l^2 = 3y_l^2$, $x_l^2 + y_l^2 = x_T^2$.

Consider a domain in the first quadrant of the subspace, $x \leq 0$, $y \leq 0$, bounded by the x and y axes and a circular arc $E = x^2 + y^2$. No trajectories can leave the domain, except possibly through the circular arc. The time derivative of E is

$$\dot{E}/2 = \lambda r^2 + (a_1 + 2a_2)r^4 + a_3(x^6 - y^6 - 15x^4 y^2 + 15x^2 y^4) < \lambda r^2 + (a_1 + 2a_2)r^4 + 6a_3 r^6,$$

where $r^2 = x^2 + y^2$. For $E = \tilde{r}^2$ where

$$\tilde{r} = \frac{-(a_1 + 2a_2) + ((a_1 + 2a_2)^2 + 24\lambda a_3)^{1/2}}{12a_3}$$

the derivative \dot{E} is non-positive, hence trajectories are trapped in the domain. For small λ the steady states $(x_H, 0)$, $(0, x_T)$, (x_u^-, y_u^-) and (x_l, y_l) are inside the domain and therefore heteroclinic connections between some of the steady states can possibly exist.

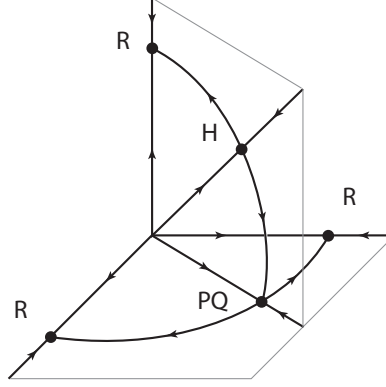


FIGURE 1. Some heteroclinic connections existing in the system (13) restricted to $\mathbf{R}^3 = (x_1, x_2, x_3)$ for $\lambda > 0$, $a_1 < 0$ and $a_2 < a_1$.

Below we assume that in (12) all branches bifurcate supercritically, in both the \mathbf{z} and \mathbf{w} subspaces, when the λ 's become positive.

Name	Typical point	Amplitude	Eigenvalues
R	$(x, 0, 0)$	$x^2 = -\lambda/a_1$	$0, 2a_1x^2, (a_2 - a_1)x^2$ (4 times)
H	(x, x, x)	$\lambda + (a_1 + 2a_2)x^2 + a_3x^4 = 0$	$0, 0, 2(a_1 + a_2)x^2, 2(a_1 - a_2)x^2$ (2 times), $-5a_3x^4$
RT	(ix, ix, ix)	$\lambda + (a_1 + 2a_2)x^2 - a_3x^4 = 0$	$0, 0, 2(a_1 + a_2)x^2, 2(a_1 - a_2)x^2$ (2 times), $5a_3x^4$
PQ	$(x, x, 0)$	$x^2 = -\lambda/(a_1 + a_2)$	$0, 0, 2(a_1 + a_2)x^2, 2(a_1 - a_2)x^2, (a_2 - a_1)x^2$ (2 times)

TABLE 1. Steady states of the normal form (13).

4.3. Heteroclinic network in \mathbf{C}^6 . The symmetry groups of single mode steady-states are given in Table 2. For each of these steady states \mathbf{C}^6 splits into a direct sum of isotypic components for the action of its symmetry group. Each of these components is an eigenspace of the linearisation of (12) near the steady state. The isotypic components and eigenvalues are presented in Tables 9 and 10. in Appendix A.

Name	Typical point	Group	Generators
R_z	$(x, 0, 0; 0, 0, 0)$	$O(2) \times (\mathbf{Z}_4 \times \mathbf{Z}_2)$	$\gamma^3, s_3; r\gamma_{\pi/2}^1; s_1$
PQ_z	$(0, x, x; 0, 0, 0)$	$\mathbf{D}_2 \times \mathbf{Z}_6$	$s_1, s_3; r\gamma_{\pi/3}^3$
H_z	$(x, x, x; 0, 0, 0)$	$\mathbf{D}_6 \times \mathbf{Z}_3$	$\rho, s_1; \gamma_{2\pi/3}^3$
T_z	$(ix, ix, ix; 0, 0, 0)$	$\mathbf{D}_6 \times \mathbf{Z}_3$	$r\rho, s_1; \gamma_{2\pi/3}^3$
R_w	$(0, 0, 0; y, 0, 0)$	$O(2) \times \mathbf{D}_4$	$\gamma^1, s_3; r\gamma_{\pi/4}^3, s_1$
PQ_w	$(0, 0, 0; 0, y, y)$	$\mathbf{D}_2 \times (\mathbf{Z}_4 \times \mathbf{Z}_2)$	$s_1, s_3; r\gamma_{\pi/2}^1, \gamma_{\pi}^2$
H_w	$(0, 0, 0; y, y, y)$	$\mathbf{D}_6 \times \mathbf{Z}_2$	$\rho, s_1; \gamma_{\pi}^1$
T_w	$(0, 0, 0; iy, iy, iy)$	$\mathbf{D}_6 \times \mathbf{Z}_2$	$r\rho, rs_1; \gamma_{\pi}^1$

TABLE 2. Symmetry groups of the steady states of the normal form (12).

From Tables 2, 9 and 10 we find 2-dimensional subspaces which are fixed by some subgroups of $\mathbf{D}_6 \times \mathbf{T}^2 \times \mathbf{Z}_2$, they are listed in Table 3. If two steady states in a 2-dimensional subspace satisfy one

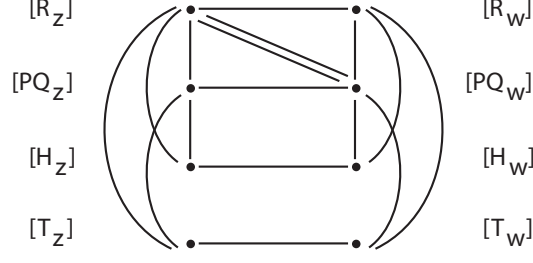


FIGURE 2. Heteroclinic connections that may exist in (12). The orientation depends on further choices in the parameters.

of the conditions ($i - iii$) of Theorem 3.1, there exists a connection between the steady states. In this way, each one of the 2-dimensional subspaces in Tables 9 and 10 gives rise to conditions for existence of a heteroclinic connection.

In subsection 4.2 connections which can exist in a single mode subspace are listed. Table 3 gives conditions for existence of connections between steady states in (\mathbf{z}) and (\mathbf{w}) subspaces. The complete heteroclinic network which may exist in the system is shown in Figure 2. We do not draw arrows showing directions of connections, because they may go either way.

Subspace	Group (generators)	Steady state	Eigenvalue
$(x, 0, 0; y, 0, 0)$	$\mathbf{D}_2 \times \mathbf{Z}_4 (s_1, s_3; \gamma_{\pi/2}^3)$	R_z	$\lambda_2 + C_4 x_R^2$
		R_w	$\lambda_1 + C_1 y_R^2$
$(x, 0, 0; 0, y, y)$	$\mathbf{D}_2 \times \mathbf{Z}_4 (s_1, s_3; r\gamma_{\pi/2}^1)$	R_z	$\lambda_2 + (C_5 + C_6)x_R^2$
		PQ_w	$\lambda_1 + (2C_2 + C_3)y_{PQ}^2$
$(x, 0, 0; 0, y, -y)$	$\mathbf{D}_2 \times \mathbf{Z}_4 (s_3, \gamma_{\pi/2}^3 s_2; r\gamma_{\pi/2}^1)$	R_z	$\lambda_2 + (C_5 - C_6)x_R^2$
		PQ_w	$\lambda_1 + (2C_2 - C_3)y_{PQ}^2$
$(0, x, x; 0, y, -y)$	$\mathbf{D}_2 (s_3, r\gamma_{\pi}^1 s_1)$	PQ_z	$\lambda_2 + (C_4 + C_5)x_{PQ}^2$
		PQ_w	$\lambda_1 + (C_1 + C_2)y_{PQ}^2$
$(x, x, x; y, y, y)$	$\mathbf{D}_6 (\rho, s_1)$	H_z	$\lambda_2 + (C_4 + 2C_5 + C_6)x_H^2$
		H_w	$\lambda_1 + (C_1 + 2C_2 + C_3)y_H^2$
$(ix, ix, ix; iy, iy, iy)$	$\mathbf{D}_6 (r\rho, r s_1)$	T_z	$\lambda_2 + (C_4 + 2C_5 - C_6)x_T^2$
		T_w	$\lambda_1 + (C_1 + 2C_2 + C_3)y_T^2$

TABLE 3. 2-dimensional fixed-point subspaces for subgroups of $\mathbf{D}_6 \times \mathbf{T}^2 \times \mathbf{Z}_2$.

5. RESTRICTION TO \mathbf{R}^6

5.1. Normal form. In what follows, we restrict our interest to $\mathbf{R}^6 = \text{Fix}(\langle s_3 \rangle)$. Since it is a fixed-point subspace, it is flow-invariant. Its Γ -orbit is a 8-dimensional subspace of \mathbf{C}^6 . The action of Γ on \mathbf{R}^6 is generated by

$$\begin{aligned}
\rho.(x_1, x_2, x_3; y_1, y_2, y_3) &= (x_2, x_3, x_1; y_2, y_3, y_1) \\
s_1.(x_1, x_2, x_3; y_1, y_2, y_3) &= (x_1, x_3, x_2; y_1, y_3, y_2) \\
r.(x_1, x_2, x_3; y_1, y_2, y_3) &= -(x_1, x_2, x_3; y_1, y_2, y_3) \\
\gamma_{\pi}^1.(x_1, x_2, x_3; y_1, y_2, y_3) &= (x_1, -x_2, -x_3; y_1, y_2, y_3) \\
\gamma_{\pi}^2.(x_1, x_2, x_3; y_1, y_2, y_3) &= (-x_1, -x_2, x_3; y_1, y_2, y_3).
\end{aligned}$$

The group action in \mathbf{R}^6 is that of $\tilde{\Gamma} = \mathbf{D}_3 \times \mathbf{Z}_2 \times \mathbf{Z}_2 = N(\langle s_3 \rangle) / \langle s_3 \rangle$, where the element of order 3 is ρ . The action of $\mathbf{D}_6 \times \mathbf{T}^2$ reduces to $\mathbf{D}_3 \times \mathbf{Z}_2$ since the γ_{α}^i , with $\alpha \neq \pi$ do not map the space to itself, s_2 acts as s_1 , s_3 acts as the identity and $\rho^2 \gamma_{\pi}^2 \rho = \gamma_{\pi}^1$.

The restriction to \mathbf{R}^6 has the advantage that $\tilde{\Gamma}$ is a discrete group. However, this leads to *hidden symmetries*: elements of Γ that do not map \mathbf{R}^6 into itself but that map some point in \mathbf{R}^6 back into \mathbf{R}^6 . This creates additional invariant subspaces, fixed by hidden symmetries but not by elements of $\tilde{\Gamma}$. It also

creates additional symmetries in some subspaces: for instance, in certain fixed-point subspaces we have $\gamma_{2\pi/4}^1$ or $\gamma_{2\pi/4}^2$ as additional symmetries, and in other subspaces we have the symmetries

$$\gamma_\alpha^3 \equiv \gamma_\alpha^1 \gamma_{-2\alpha}^2 \cdot (x_1, x_2, x_3; y_1, y_2, y_3) = (x_1, e^{-3i\alpha} x_2, e^{3i\alpha} x_3; e^{-4i\alpha} y_1, e^{2i\alpha} y_2, e^{2i\alpha} y_3)$$

with α one of $0, \pi/3, \pi/5, \pi/6$, etc. These are not elements of $\tilde{\Gamma}$, but have to be taken into account in the analysis.

The vector field restricted to \mathbf{R}^6 is as follows:

$$(21) \quad \begin{cases} \dot{x}_1 = x_1[\lambda_1 + A_1 x_1^2 + A_2(x_2^2 + x_3^2) + C_1 y_1^2 + C_2(y_2^2 + y_3^2)] + A_3 x_1 x_2^2 x_3^2 + C_3 x_1 y_2 y_3 \\ \dot{x}_2 = x_2[\lambda_1 + A_1 x_2^2 + A_2(x_1^2 + x_3^2) + C_1 y_2^2 + C_2(y_1^2 + y_3^2)] + A_3 x_1^2 x_2 x_3^2 + C_3 x_2 y_1 y_3 \\ \dot{x}_3 = x_3[\lambda_1 + A_1 x_3^2 + A_2(x_1^2 + x_2^2) + C_1 y_3^2 + C_2(y_1^2 + y_2^2)] + A_3 x_1^2 x_2^2 x_3 + C_3 x_3 y_1 y_2 \\ \dot{y}_1 = y_1[\lambda_2 + B_1 y_1^2 + B_2(y_2^2 + y_3^2) + C_4 x_1^2 + C_5(x_2^2 + x_3^2)] + B_3 y_1 y_2^2 y_3^2 + C_6(y_2 x_3^2 + y_3 x_2^2) \\ \dot{y}_2 = y_2[\lambda_2 + B_1 y_2^2 + B_2(y_1^2 + y_3^2) + C_4 x_2^2 + C_5(x_1^2 + x_3^2)] + B_3 y_1^2 y_2 y_3^2 + C_6(y_3 x_1^2 + y_1 x_3^2) \\ \dot{y}_3 = y_3[\lambda_2 + B_1 y_3^2 + B_2(y_1^2 + y_2^2) + C_4 x_3^2 + C_5(x_1^2 + x_2^2)] + B_3 y_1^2 y_2^2 y_3 + C_6(y_1 x_2^2 + y_2 x_1^2). \end{cases}$$

In Boussinesq convection with rigid or stress-free horizontal boundaries stable rolls exist at the onset of convection [9]. Respectively, in what follows we assume $\lambda_1 > 0, \lambda_2 > 0, A_1 < 0, B_1 < 0, A_2 < A_1$ and $B_2 < B_1$. Under this assumption only two types of equilibria may be involved in a heteroclinic network. These are rolls (R) and patchwork quilts (PQ). (A trajectory can not reach hexagons or triangles, see sections 4.1, 4.2 and Figures 1 and 2) Alternative representations for these patterns that do not lie in the same $\tilde{\Gamma}$ -orbit are indicated with a tilde. We shall need

$$\widetilde{PQ}_w = (0, 0, 0; y, -y, 0) = \gamma_{\pi/2}^3 \cdot PQ_w$$

where $\gamma_{\pi/2}^3$ is a hidden symmetry acting on the space $\{(x_1, 0, 0; y_1, y_2, y_3)\} = \text{Fix}(\langle \gamma_\pi^1 \rangle)$.

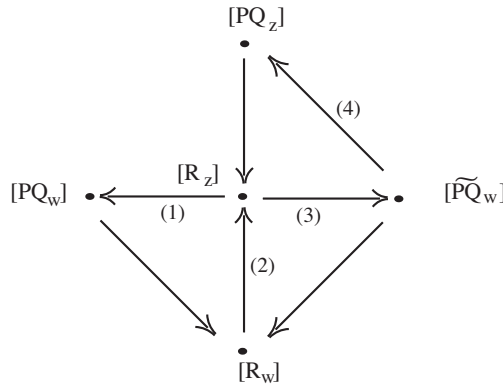
6. NETWORK IN \mathbf{R}^6

The aim of this section is to establish the conditions for existence of a heteroclinic network in \mathbf{R}^6 involving rolls and patchwork quilts in the two modes. The network is persistent under small perturbations that preserve the underlying symmetries.

In general a connection $X \rightarrow Y$ is persistent if the two invariant manifolds meet transversely. In equations with symmetry there is another source of persistence: a saddle-sink connection inside a 2-dimensional fixed-point subspace cannot be broken by perturbations that preserve the symmetry, as will be the case here.

6.1. Quotient network. In the next result, $[X]$ denotes the group orbit class of X under the action of $\tilde{\Gamma} = \mathbf{D}_3 \times \mathbf{Z}_2 \times \mathbf{Z}_2$. We show the existence of a quotient heteroclinic network.

Theorem 6.1. *There is an open set of parameters for which the equations (21) have a persistent heteroclinic network with the following architecture:*



The open set of parameters is given by the conditions of Table 4 below.

The quotient heteroclinic network of Theorem 6.1 is made of three heteroclinic cycles. Cycle C_{12} involving equilibria $[R_z], [R_w]$ and $[PQ_w]$, cycle C_{23} involving equilibria $[R_z], [R_w]$ and $[\widetilde{PQ}_w]$, and cycle C_{34} involving equilibria $[R_z], [PQ_z]$ and $[\widetilde{PQ}_w]$. Note that cycles C_{12} and C_{23} constitute a subnetwork

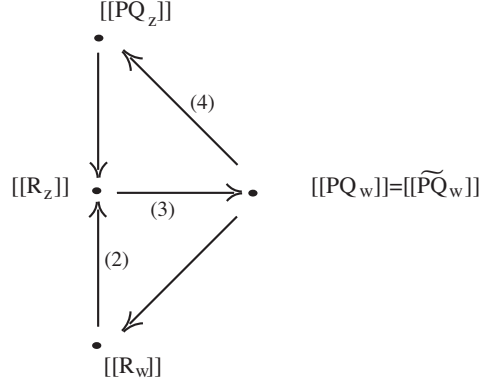
A_j	B_j	C_j	$\lambda_1 > 0$ and $\lambda_2 > 0$
$A_2 < A_1 < 0$	$B_2 < B_1 < 0$	$C_4 < 0$	$\lambda_1/\lambda_2 > A_1/C_4$ $\lambda_1/\lambda_2 > C_1/B_1$
		$2C_2 + C_3 < 0$	$\lambda_1/\lambda_2 < (2C_2 + C_3)/(B_1 + B_2)$
		$2C_2 - C_3 < 0$	$\lambda_1/\lambda_2 < (2C_2 - C_3)/(B_1 + B_2)$
			$\lambda_2/\lambda_1 > (C_5 + C_6)/A_1$ $\lambda_2/\lambda_1 > (C_5 - C_6)/A_1$

TABLE 4. Conditions on parameters for existence of the network of Theorem 6.1. Reversing some of the inequalities will produce connections in the opposite direction.

which we shall denote by Σ_{123} . Another subnetwork, denoted Σ_{234} , is made of cycles C_{23} and C_{34} . These two subnetworks have cycle C_{23} in common.

The existence of a network for the equations in \mathbf{C}^6 follows immediately from Theorem 6.1. Denoting by $[[X]]$ the equivalence class of X under the action of $\Gamma = \mathbf{D}_6 \times \mathbf{T}^2 \times \mathbf{Z}_2$ we have:

Corollary 6.2. *There is an open set of parameters for which the equations (12) have a heteroclinic network with the following architecture:*



The open set of parameters is given by the conditions of Table 4.

With the additional assumptions $C_5 + C_6 < 0$ and $C_5 - C_6 < 0$ the conditions in Table 4 take the simpler form of Table 5.

A_j	B_j	C_j	λ_1/λ_2	$\lambda_1 > 0, \lambda_2 > 0$
$A_2 < A_1 < 0$	$B_2 < B_1 < 0$	$C_4 < 0$	$\lambda_1/\lambda_2 > A_1/C_4$ $\lambda_1/\lambda_2 > C_1/B_1$	
		$2C_2 + C_3 < 0$	$\lambda_1/\lambda_2 < (2C_2 + C_3)/(B_1 + B_2)$	
		$2C_2 - C_3 < 0$	$\lambda_1/\lambda_2 < (2C_2 - C_3)/(B_1 + B_2)$	
		$C_5 + C_6 < 0$	$\lambda_1/\lambda_2 < A_1/(C_5 + C_6)$	
		$C_5 - C_6 < 0$	$\lambda_1/\lambda_2 < A_1/(C_5 - C_6)$	

TABLE 5. Simpler conditions on parameters for existence of the network of Theorem 6.1.

The proof of Theorem 6.1 consists of exhibiting conditions on the parameters and representatives of the nodes for which the connections exist. The nodes are written with the convention $x > 0, y > 0$ as:

$$\begin{array}{lll}
R_z & = & (x, 0, 0; 0, 0, 0) \quad \rho R_z & = & (0, 0, x; 0, 0, 0) \quad \rho^2 R_z & = & (0, x, 0; 0, 0, 0) \\
PQ_z & = & (x, x, 0; 0, 0, 0) \quad \rho PQ_z & = & (x, 0, x; 0, 0, 0) \quad \rho^2 PQ_z & = & (0, x, x; 0, 0, 0) \\
R_w & = & (0, 0, 0; y, 0, 0) \quad \rho R_w & = & (0, 0, 0; 0, 0, y) \quad \rho^2 R_w & = & (0, 0, 0; 0, y, 0) \\
PQ_w & = & (0, 0, 0; y, y, 0) \quad \rho PQ_w & = & (0, 0, 0; y, 0, y) \quad \rho^2 PQ_w & = & (0, 0, 0; 0, y, y) \\
\widetilde{PQ}_w & = & (0, 0, 0; y, -y, 0) \quad \rho \widetilde{PQ}_w & = & (0, 0, 0; -y, 0, y) \quad \rho^2 \widetilde{PQ}_w & = & (0, 0, 0; 0, y, -y).
\end{array}$$

Some of their r -conjugates, indicated as $-PQ_w$, $-\rho\widetilde{PQ}_w$, etc, correspond to the choices $x < 0$ or $y < 0$.

The proof of Theorem 6.1 consists in finding for each connection a two-dimensional fixed-point subspace that contain representatives of the two equilibria involved, as was indicated in subsection 4.2 plus an application of one of the cases of Theorem 3.1, and checking the conditions it imposes on the coefficients. For the single-mode connections listed in Table 6 the necessary conditions are $\lambda_1 > 0$ and $\lambda_2 > 0$, $A_2 < A_1 < 0$ and $B_2 < B_1 < 0$.

connection	representative	subspace	isotropy s_3 and
$[PQ_z] \rightarrow [R_z]$	$PQ_z \rightarrow R_z, PQ_z \rightarrow \rho^2 R_z$	$(x_1, x_2, 0; 0, 0, 0)$	$r\gamma_\pi^2$
$[PQ_w] \rightarrow [R_w]$	$PQ_w \rightarrow R_w, PQ_w \rightarrow \rho^2 R_w$	$(0, 0, 0; y_1, y_2, 0)$	$\gamma_\pi^1, r\gamma_{\pi/2}^2, r\gamma_{3\pi/2}^2$
$[\widetilde{PQ}_w] \rightarrow [R_w]$	$\widetilde{PQ}_w \rightarrow R_w, \widetilde{PQ}_w \rightarrow -\rho^2 R_w$		

TABLE 6. Fixed-point subspaces and representatives for single mode connections in Theorem 6.1 and subsection 4.2.

Connections between patterns of different modes are listed in Table 7 the necessary conditions are $\lambda_1 > 0$ and $\lambda_2 > 0$, and for A_j, B_j, C_j either the conditions of Table 4 or those of Table 5.

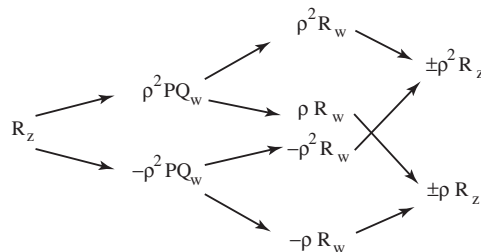
connection	representative	subspace	isotropy s_3 and
$[R_w] \rightarrow [R_z]$	$R_w \rightarrow \pm R_z$	$(x_1, 0, 0; y_1, 0, 0)$	$\gamma_\pi^1, s_1, \gamma_{\pi/2}^3$
$[R_z] \rightarrow [PQ_w]$	$R_z \rightarrow \pm\rho^2 PQ_w$	$(x_1, 0, 0; 0, y_2, y_2)$	$\gamma_\pi^1, s_1, r\gamma_{\pi/2}^1$
$[R_z] \rightarrow [\widetilde{PQ}_w]$	$R_z \rightarrow \pm\rho^2 \widetilde{PQ}_w$	$(x_1, 0, 0; 0, y_2, -y_2)$	$\gamma_\pi^1, s_1 r\gamma_\pi^2$
$[\widetilde{PQ}_w] \rightarrow [PQ_z]$	$\rho^2 \widetilde{PQ}_w \rightarrow \pm\rho^2 PQ_z$	$(0, x_2, x_2; 0, y_2, -y_2)$	$s_1 r\gamma_\pi^1$

TABLE 7. Fixed-point subspaces and representatives for mixed mode connections in Theorem 6.1 and subsection 4.2.

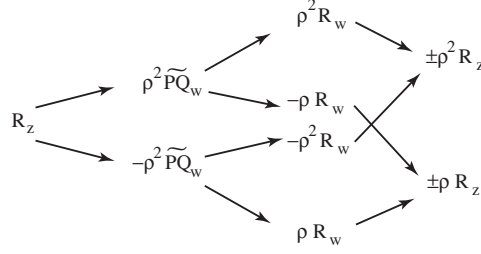
6.2. Motifs and cycles. We are interested in heteroclinic cycles formed by *primary connections* — those taking place as a saddle-to-sink connection inside an invariant plane. In order to recover the cycles in \mathbf{R}^6 from the network architecture of Theorem 6.1 we need some additional information. This is because when we indicate a connection $[X] \rightarrow [Y]$, in the quotient network, it does not mean that there is a primary connection from all representatives of X to all representatives of Y . The complete information is encoded in *motifs* that show all the primary connections effectively followed along a cycle in the quotient network for a given starting point. Since R_z is a representative of the node shared by the three cycles, we write all motifs starting at R_z and ending at a conjugate of R_z , for simplicity. Cycles in \mathbf{R}^6 may then be formed by concatenating a path in a motif to a path in the motif's image by a suitable element of $\widetilde{\Gamma}$.

Proposition 6.3. *Complete motifs in \mathbf{R}^6 for the quotient cycles C_{12} , C_{23} and C_{34} starting at R_z and containing all the primary connections, are the following:*

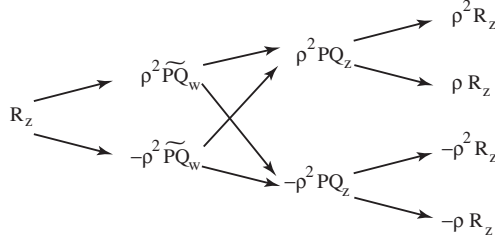
C_{12} motif:



C_{23} motif:



C_{34} motif:



Moreover, all the paths in the motif for C_{12} are conjugated by $\tilde{\Gamma}$, all those in the motif for C_{23} are conjugated by $\tilde{\Gamma}$ plus a hidden symmetry. The paths in the motif for C_{34} lie in two different Γ orbits.

Proof. The connections in the motifs are those in Tables 6 and 7. It remains to see, for each node and each motif, that there are no other primary connections following that cycle. In the case of C_{12} , for instance, there are three planes containing R_z that also intersect the orbit $[PQ_w]$. The planes $(x_1, 0, 0; y_1, 0, y_1)$ and $(x_1, 0, 0; y_1, y_1, 0)$ are not flow-invariant, so the only primary connections starting at R_z and of the form $[R_z] \rightarrow [PQ_w]$ are those in $Fix(s_3, \gamma_\pi^1, s_1, r\gamma_\pi^1/2) = \{(x_1, 0, 0; 0, y_1, y_1)\}$. Similar arguments may be used for the other nodes in C_{12} and for the other cycles.

Finally, the subgroup of $\tilde{\Gamma}$ generated by s_1 , γ_π^1 and $r\gamma_\pi^1/2$ maps the path $R_z \rightarrow \rho^2 PQ_w \rightarrow \rho^2 R_w \rightarrow \rho^2 R_z$ into the other paths in the motif for C_{12} . The paths in the motif for C_{23} are interchanged by the same subgroup. Symmetries mapping the motif for C_{34} into itself are s_1 and γ_π^1 . \square

To generate a heteroclinic cycle in \mathbf{R}^6 we start with a path in one of the motifs ending at δR_z , then we concatenate it to a path in the δ image of the motif. Note that no motif starting at R_z ends at $\pm R_z$.

Corollary 6.4. *There is an open set of parameters for which the equations (21) have a heteroclinic network of primary connections. For all cycles in the network the number of nodes is a multiple of 3, with a minimum of 6.*

Examples of cycles generated by paths in the motifs in Proposition 6.3 are given in Figures 3–6 below.

6.3. Cycles in the network. Consider the path

$$R_z \rightarrow \rho^2 PQ_w \rightarrow \rho R_w \rightarrow \rho R_z$$

in the motif for C_{12} in Proposition 6.3. In order to build a cycle from it, we must take now a path in the ρ -conjugate of the motif. One choice is to take the ρ -conjugate of the same path, that will end with $\rho^2 R_z$ and then the ρ^2 -conjugate of the path that will close the cycle. This yields a 9-node cycle that is mapped into itself by ρ , shown in Figure 3, together with a numerical simulation of a trajectory that follows this cycle.

Figure	A_1	A_2	A_3	B_1	B_2	B_3	C_1	C_2	C_3	C_4	C_5	C_6
3	-1.5	-2.2	0.015	-2.	-2.6	0.02	10.5	-15.	-2.8	-5.5	-2.9	0.05
4	-1.5	-2.2	0.015	-2.	-2.6	0.02	10.5	-15.	-2.8	-5.5	-2.9	-0.05
5	-2.5	-4.2	0.015	-2.	-2.6	0.02	1.7	-2.5	0.4	-25.5	-11.7	-9.5
6	-2.5	-4.2	0.015	-2.	-2.2	0.02	1.8	-2.5	0.2	-35.	-37.	-47.

TABLE 8. Parameter values for Figures 3, 4, 5 and 6, $\lambda_1 = 1$, $\lambda_2 = 2$ in all.

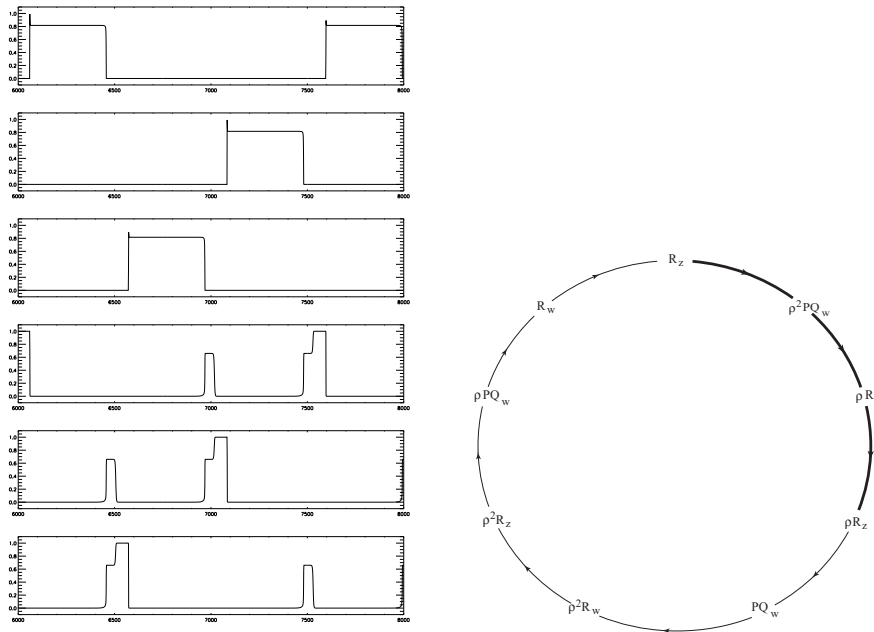


FIGURE 3. **Left:** time series for $x_1, x_2, x_3; y_1, y_2, y_3$ (from top to bottom) for numerical simulations of solutions following the quotient cycle C_{12} . Parameter values in Table 8. Initial condition $(.63, .00002, .000012, .00001, .000005, .000015)$. **Right:** The trajectory follows this 9-node cycle, generated by the ρ -orbit of a path (thicker arrows) in the motif for C_{12} .

If we take ρ -conjugates of the path

$$R_z \rightarrow \rho^2 \widetilde{PQ}_w \rightarrow -\rho R_w \rightarrow \rho R_z$$

in the motif for C_{23} in Proposition 6.3, we generate a 9-node cycle. An 18-node cycle may be created by concatenating the path to the ρ -conjugate of another path in the same motif, like the $r\gamma_\pi^2$ -conjugate:

$$R_z \rightarrow -\rho^2 \widetilde{PQ}_w \rightarrow \rho R_w \rightarrow \rho R_z.$$

Since $\rho r\gamma_\pi^2$ has order 6, when we add to the end of each path its $\rho r\gamma_\pi^2$ -conjugate we obtain the 18-node cycle shown in Figure 4 with a numerical simulation of a trajectory following the cycle. Note that the cycle goes twice through each node in the ρ -orbit of R_z , since R_z is fixed by $r\gamma_\pi^2$.

The two cycles in Figures 3 and 4 share the nodes R_z, R_w and their ρ - and ρ^2 -conjugates, forming a subnetwork. Conjugating the cycle in Figure 4 by $r\gamma_\pi^2$ we obtain another 9-node cycle that shares the nodes $\rho^j R_z$ with the first two cycles, and $-\rho^j R_w$ with the 18-node cycle.

A minimal cycle, as in Corollary 6.4, may be obtained concatenating

$$R_z \rightarrow \rho^2 \widetilde{PQ}_w \rightarrow -\rho R_w \rightarrow \rho R_z$$

to its ρs_1 -conjugate. This is the same path in the quotient cycle C_{23} used to generate the 18-node cycle in Figure 4, but this time it generates a 6-node cycle, using a symmetry of order 2. The 6-node cycle is shown in Figure 5, where it should be noted that $s_1 \widetilde{PQ}_w = -\widetilde{PQ}_w$ and $s_1 \rho R_w = R_w$. The trajectory in the numerical simulation goes round this cycle twice in the time series shown.

A more irregular cycle is generated from the motif for C_{23} as follows: start with the path

$$R_z \rightarrow \rho^2 \widetilde{PQ}_w \rightarrow \rho R_w \rightarrow \rho^2 R_z$$

and add its conjugate by $r\rho^2\gamma_\pi^2$ to form a 6-node path starting with R_z and ending with ρR_z . Then add the ρ and ρ^2 conjugates of the 6-node path to form an 18-node cycle. The cycle and a trajectory that follows it are shown in Figure 6.

In section 7 we discuss how nearby trajectories follow these cycles, as in the numerics shown here.

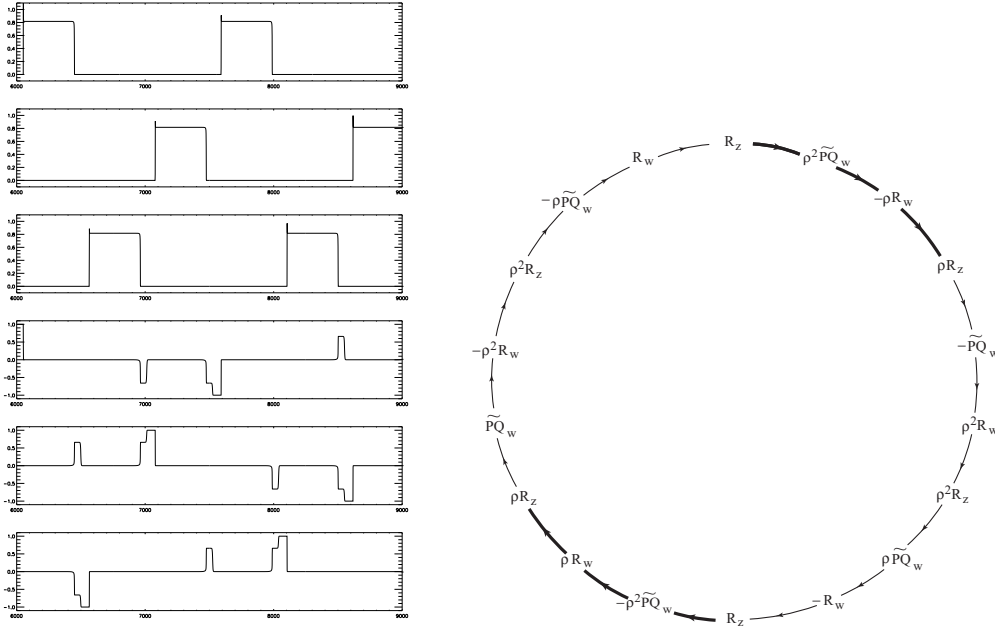


FIGURE 4. **Left:** time series for $x_1, x_2, x_3; y_1, y_2, y_3$ (from top to bottom) for numerical simulations of solutions following the quotient cycle C_{23} . Parameter values in Table 8. All parameters and also the initial condition are the same as in Figure 3, except for C_6 that changes sign. **Right:** The trajectory follows this 18-node cycle. The generating path and its $r\gamma_\pi^2$ -conjugate are shown with thicker arrows.

7. DYNAMICS NEAR THE NETWORK

In this section we describe the behaviour of trajectories starting close to the network of Section 6. Our aim is to predict what might be observed numerically or in an experiment modelled by these equations. We start by the local behaviour near a *branch point*: a node X_B where two connections go out. We show there is always switching at branch points: there are trajectories following each connection going away from X_B . For some branch points there are more initial conditions following one of the connections. This is controlled by the parameters in the equation in a way similar to railroad switches: the parameters choose which track is going to be used.

7.1. Switching at a node. Consider a splitting of $\mathbf{R}^{n+m} = E^n \oplus E^m$ into vector subspaces E^n and E^m of dimensions n and m and let $B^n(\varepsilon)$ denote a ball of radius ε in E^n . An n -dimensional disk D_ε^n of radius ε is the graph of a smooth map $h : B^n(\varepsilon) \rightarrow B^m(\varepsilon)$. In particular, at a hyperbolic equilibrium the local stable and unstable manifolds W_{loc}^s and W_{loc}^u are disks. When the reference to the radius ε is irrelevant we write D^n for the disk.

Let X, Y be equilibria of a vector field with flow $\varphi(t, p)$. Given a neighbourhood V_X of X we say a point $p \in V_X$ follows the connection $X \rightarrow Y$ in V_X with distance $\varepsilon > 0$ if there is a $\tau > 0$ such that $\varphi(t, p) \in V_X$ for all $t \in [0, \tau]$ and such that $\varphi(\tau, p)$ lies at a distance less than ε to the connection $X \rightarrow Y$.

Consider the following connections for a vector field in \mathbf{R}^m :

$$(22) \quad \begin{array}{ccc} & & X_1 \\ & \nearrow & \\ X_0 & \rightarrow & X_B \\ & \searrow & \\ & & X_2 \end{array}$$

We say there is *switching at the node X_B* if given a neighbourhood V_{X_B} of X_B , for any $\varepsilon > 0$, and for any disk D^{n-1} that meets the connection $X_0 \rightarrow X_B$ transversally at a point in V_{X_B} there are points in D^{n-1} that follow each of the connections $X_B \rightarrow X_1$ and $X_B \rightarrow X_2$ in V_{X_B} with distance ε .

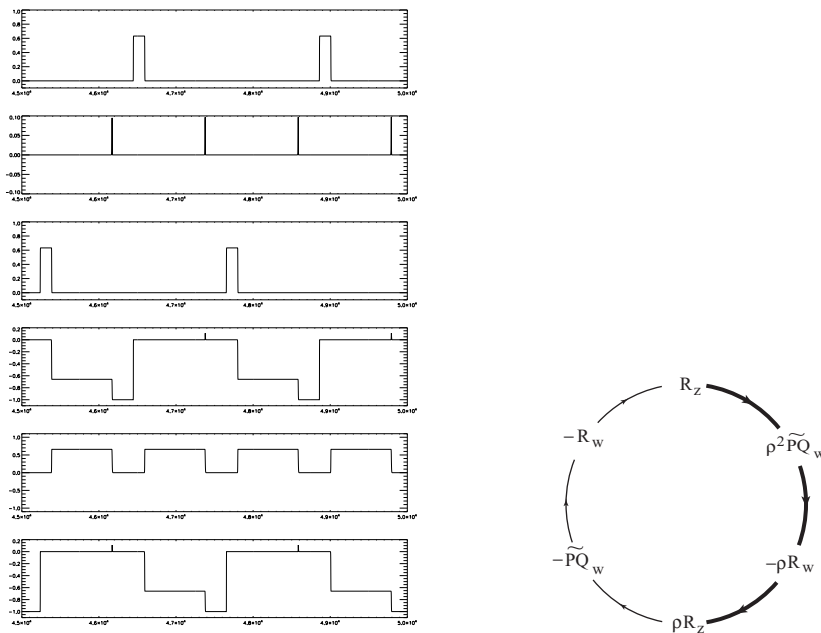


FIGURE 5. **Left:** time series for $x_1, x_2, x_3; y_1, y_2, y_3$ (from top to bottom) for numerical simulations of solutions following the quotient cycle C_{23} . Parameter values in Table 8. The peaks in the x_2 time series are transients and do not correspond to any equilibrium in the equations, as may be seen by noting that their size is the same as the tiny peaks in the time series for y_1 and y_3 , occurring at the same times. **Right:** The trajectory goes twice around this minimal 6-node cycle, generated by the path in thicker arrows and its conjugate by a symmetry of order 2.

Proposition 7.1. *In a motif containing the connections (22) between hyperbolic nodes, there is always switching at the node X_B .*

Proof. Let m be the dimension of the stable manifold of X_B , let D^{n-1} be a disk that meets the connection $X_0 \rightarrow X_B$ transversally and let V_{X_B} be a neighbourhood of X_B . By the flow-box theorem, D^{n-1} contains a lower dimensional disk that is mapped by the flow, after a sufficient time $t > 0$, into a disk D^{n-m} contained in V_{X_B} and transverse to $W_{loc}^s(X_B)$. Thus, it is sufficient to establish that points in D^{n-m} follow the two connections. By the λ -Lemma for flows (Corollary 3.2 in [8]), there are constants $\tau > 0$ and $C > 0$ such that for every $t \geq \tau$ the image $\varphi(t, D^{n-m})$ is C^k exponentially close to $W_{loc}^u(X_B)$ by $Ce^{-\lambda t}$. Therefore it contains points close to both connections. \square

All the nodes in the motifs of Proposition 6.3 are branch points. They are hyperbolic for most values of the parameters for which the connections exist: lack of hyperbolicity means that the parameters satisfy some extra equalities, defining subsets of codimension 1 in parameter space. Therefore we have:

Corollary 7.2. *There is switching at all nodes in the motifs of Proposition 6.3 and their conjugates, for almost every parameter value for which the connections exist.*

7.2. Railroad switches. In general, when the connections at a branch point take place in non conjugate fixed-point subspaces one of them is preferred by most nearby trajectories. We make this statement precise in this section.

If the two connections leaving the branch point X_B in the motif (22) take place in non conjugate fixed-point subspaces, then generically they will correspond to different positive eigenvalues of the linearisation at X_B of the vector field. Suppose also that the linearisation of the vector field may be represented by a diagonal matrix after a linear change of coordinates. When this happens and moreover all the other eigenvalues are real and negative, we say there is a *railroad switch* at the branch point X_B .

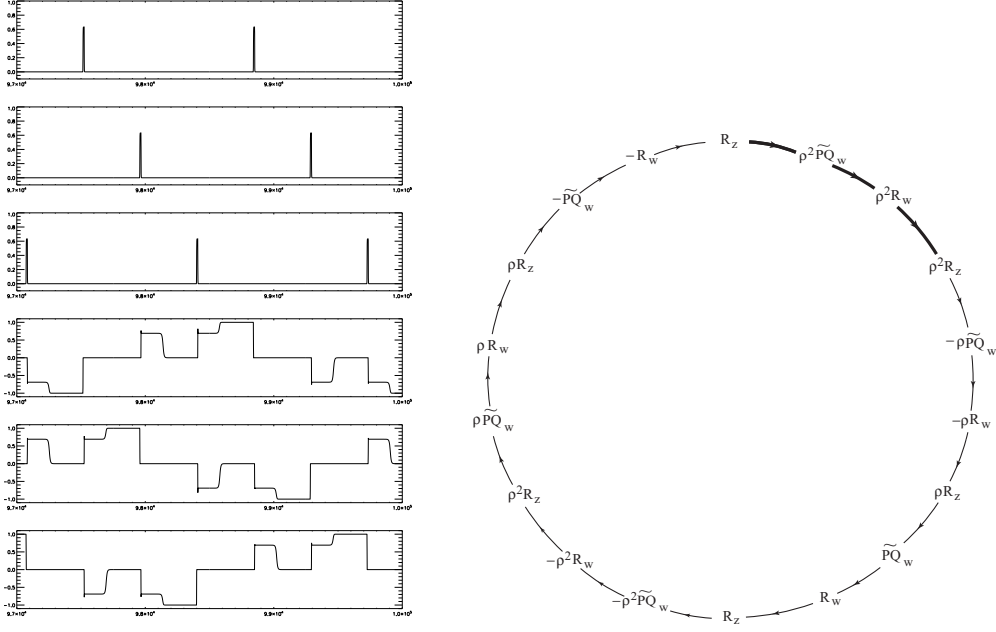


FIGURE 6. **Left:** time series for $x_1, x_2, x_3; y_1, y_2, y_3$ (from top to bottom) for numerical simulations of solutions following the quotient cycle C_{23} . Parameter values in Table 8. **Right:** The trajectory follows this 18-node cycle, generated by the third order symmetry ρ applied to the path in thicker arrows and its $r\rho^2\gamma_\pi^2$ conjugate.

We will denote the eigenvalues at the branch point X_B as

$$(23) \quad -\nu_4 \leq -\nu_3 \leq -\nu_2 \leq -\nu_1 < 0 < \mu_1 < \mu_2$$

where μ_j is the eigenvalue in the subspace containing the connection $X_B \rightarrow X_j$.

Given a disk D^2 transverse to the stable manifold of X_B we want to describe the set of initial conditions in D^2 that follow each of the connections starting at such a branch point. Using Proposition 7.1, we may assume that D^2 is already very close to the unstable manifold of X_B .

Consider the linear equations:

$$(24) \quad \begin{cases} \dot{v}_l = \mu_l v_l & l = 1, 2 \\ \dot{u}_j = -\nu_j u_j & j = 1, \dots, 4 \end{cases}$$

By Samovol's theorem [23] (see also Section 6.4, Ch 3, Part I of [4]) there is a C^1 change of coordinates mapping the flow in a neighbourhood V_B of X_B into that of (24). In the new coordinates the point X_B is the origin, $W_{loc}^s(X_B)$ is the subspace $\{v_1 = v_2 = 0\}$, the unstable manifold $W_{loc}^u(X_B)$ is the plane $\{u_j = 0, j = 1, \dots, 4\}$ and the connections $X_B \rightarrow X_l, l = 1, 2$ take place along the v_l axes.

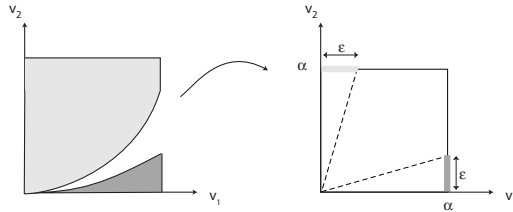


FIGURE 7. Trajectories starting on the shadowed areas on the left follow the connections $X_B \rightarrow X_1$ and $X_B \rightarrow X_2$, going through the ε -neighbourhoods of the axes on the square (right). Points in the light grey area are mapped close to the v_2 axes, those in the darker area stay near the v_1 axis.

Let \mathcal{Q} be a square $\{|v_l| \leq \alpha, l = 1, 2, u_j = 0, j = 1, \dots, 4\}$, contained in V_B and let $v_1(t), v_2(t)$ be the first two coordinates of a trajectory that starts at a disk D^2 transverse to $W_{loc}^s(X_B)$. Trajectories that follow the connection $X_B \rightarrow X_1$ at a distance $\varepsilon > 0$ pass the boundary of \mathcal{Q} close to the v_1 -axis (Figure 7). These trajectories satisfy $|v_2(t)| < \varepsilon$ at the time t when $v_1(t) = \pm\alpha$. For $v_1(0) = v_1^0 > 0, v_2(0) = v_2^0 > 0$ this means $v_2^0 < \varepsilon(v_1^0/\alpha)^{\mu_2/\mu_1}$, a cusp-shaped region bounded by the v_1 axis and by a curve tangent to it. Similarly, trajectories following $X_B \rightarrow X_2$ at a distance $\varepsilon > 0$ close to the boundary of \mathcal{Q} have initial conditions $v_1^0 > 0, v_2^0 > 0$ in a larger region $v_2^0 > \alpha(v_1^0/\varepsilon)^{\mu_2/\mu_1}$ bounded by the v_2 axis and a curve tangent to the v_1 axis (Figure 7). The picture in the other quadrants may be obtained by reflection on the axes. We have proved:

Proposition 7.3. *Consider a motif of the form (22) with a railroad switch at X_B . Then most nearby trajectories will follow the connection that corresponds to the largest eigenvalue.*

Consider the square $\mathcal{Q}_\eta = \{0 \leq v_l \leq \eta, l = 1, 2\}$ in D_η^2 and inside it the region S_η containing initial conditions that follow the connection $X_B \rightarrow X_2$ and arrive at the segment $v_2 = \alpha$ at a distance ε to the v_2 axis, as in the construction above (light grey area in Figure 7). From the expressions used for Proposition 7.3, it follows that the ratio of the areas of S_η to \mathcal{Q}_η satisfies

$$\frac{L(S_\eta)}{L(\mathcal{Q}_\eta)} = 1 - \frac{\mu_1}{\mu_1 + \mu_2} \alpha \varepsilon^{-\mu_2/\mu_1} \eta^{-1 + \mu_2/\mu_1} \implies \lim_{\eta \rightarrow 0} \frac{L(S_\eta)}{L(\mathcal{Q}_\eta)} = 1$$

where L is the Lebesgue measure on D_η^2 . In this sense, finding trajectories that follow the connection $X_B \rightarrow X_2$ is a lot more probable than finding those that follow $X_B \rightarrow X_1$ and we say then that there is *essentially no switching* at X_B .

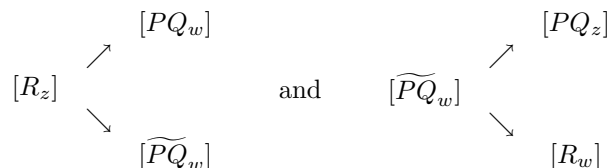
This property is preserved if the change of coordinates guaranteed by Samovol's theorem is of class C^2 , but this requires the fulfilment of some non-resonance conditions that may be difficult to obtain in equations with symmetry. The non-resonance conditions for a C^1 change of coordinates are automatically satisfied with the eigenvalues in (23). Incorporating the second order non-resonance conditions, all of which concern the negative eigenvalues $\nu_l, l = 1, \dots, 4$, we have:

Proposition 7.4. *Suppose that at the branch point X_B in the motif (22), with a railroad switch at X_B , the eigenvalues (23) do not have any of the following resonances:*

$$\begin{aligned} \nu_2 = 2\nu_1 \quad \nu_3 = 2\nu_1 \quad \nu_4 = 2\nu_1 \\ \nu_1 = \nu_2 \quad \text{and} \quad \nu_4 = 2\nu_3 \\ \nu_1 = \nu_2 \quad \text{and} \quad \nu_4 = \nu_3 + \nu_2 \end{aligned}$$

Then there is *essentially no branching* at X_B .

Railroad switches appear in many previous articles, in particular, Kirk and Silber [12], Brannath [6] and Aguiar and Castro [1]. The preferred connection may be controlled by parameters in the equations that change the relative size of the eigenvalues. In our case this will arise at branch points of the following types



where connections take place in different subspaces. At all other branch points in the motifs of Proposition 6.3 the pairs of connections take place along the same eigenspace, so there is no railroad switch there. Nearby trajectories may be equally distributed between the two connections.

A railroad switch accounts for the differences in Figures 3 and 4 that show numerical plots of two trajectories with the same initial condition, where the only difference is a change in sign of a parameter that controls the relative size of the eigenvalues at the branch point. The trajectory in Figure 3 follows consistently the connections $[R_z] \rightarrow [PQ_w]$, while that of Figure 4 follows $[R_z] \rightarrow [\widetilde{PQ}_w]$.

7.3. Stability of cycles. Given a quotient cycle, the union of all the cycles that may be obtained by concatenating paths in the corresponding motif and in its conjugates, forms a subnetwork that we will also call a heteroclinic cycle. These cycles cannot be asymptotically stable, since at some of their nodes there are connections that move away from them, but they may still attract a large set of nearby trajectories.

The Krupa-Melbourne [13, 14] criteria for asymptotic stability of heteroclinic cycles are not applicable here. This is not surprising, since the criteria imply asymptotic stability and this is not possible in a network. Note that the criterium in [13] needs one-dimensional unstable manifolds at the nodes, and for the criterium in [14] it is asked that the unstable manifold of each node is contained in the group orbit of the stable manifold of the next node in the cycle. We adapt the Krupa-Melbourne [?, 14] and Brannath [6] proofs to obtain a weaker form of stability.

Given a disk D_η transverse to a connection $X_0 \rightarrow X_B$ in a cycle where there is a railroad switch at X_B , consider the set $S_\eta \subset D_\eta$ of points whose trajectories follow the connections in the cycle with distance $\varepsilon > 0$ up to another connection $\gamma X_0 \rightarrow \delta X_B$, for some $\gamma, \delta \in \tilde{\Gamma}$. We say that the cycle is *essentially stable* if for small $\varepsilon > 0$ we have

$$\lim_{\eta \rightarrow 0} \frac{L(S_\eta)}{L(D_\eta)} = 1$$

where L is the Lebesgue measure. The cycle is *essentially asymptotically stable* if a similar property also holds for the set of points in D_η whose trajectories approach the cycle as $t \rightarrow \infty$.

Theorem 7.5. *The cycle C_{12} is essentially asymptotically stable in \mathbf{R}^6 for a non empty open set of parameter values for which the cycles C_{12} and C_{23} coexist.*

Proof. We will impose conditions on the parameters to ensure the coexistence of the cycles and the essential stability of C_{12} . First we state the conditions and explain why they hold on a non empty open set, then we show how they imply the stability.

We start with the conditions of Section 6 for existence of the connections in C_{12} and C_{23} . To these we add the condition that all the eigenvalues at the nodes $[R_z]$, $[R_w]$, $[PQ_w]$ and $[PQ_z]$ are negative, except for those guaranteeing the connections (the eigenvalues at each node are listed in Tables 9 and 10). In order to have essentially no branching at $[R_z]$ with trajectories following the connections $[R_z] \rightarrow [PQ_w]$ we impose the non-resonance conditions in Proposition 7.4 and the condition $C_6 > 0$ to have the eigenvector in the $[PQ_w]$ direction corresponding to the largest eigenvalue at $[PQ_z]$.

Then, following the notation of [13], at each node X_j of the quotient cycle consider the eigenvalues of the derivative of the vector field at X_j and let P_j be the plane that contains the connection $X_j \rightarrow X_{j+1}$. The eigenvalue in the invariant line $P_{j_1} \cap P_j$ that contains X_j is called radial. Let e_j be the maximum positive eigenvalue, $-c_j$ be the non-radial eigenvalue in P_j and let t_j be the maximum eigenvalue whose eigenvector is not contained in $P_{j_1} + P_j$, the weakest transverse eigenvalue. We require that the Krupa-Melbourne [13] condition for stability is satisfied for C_{12} :

$$\prod_{j=1}^3 \min(c_j, e_j - t_j) > \prod_{j=1}^3 e_j.$$

These conditions define an open set of parameters, since all of them are given by inequalities. We know the open set is not empty, because the conditions are satisfied by the parameter values used for the simulation in Figure 3, given in the first row of Table 8.

Consider a neighbourhood of R_z where there is a C^2 change of coordinates transforming the differential equations into the linear form (24), where the positive half-axis v_2 corresponds to the connection $R_z \rightarrow \rho^2 PQ_w$. In these coordinates, let P_2 be the plane $u_j = u_j^0 = \text{constant}$, $j = 1, \dots, 4$, transverse to $W_{loc}^s(R_z)$ and let P_α be the hyperplane $v_2 = \alpha$, transverse to $R_z \rightarrow \rho^2 PQ_w$. As in Proposition 7.4 we look at the square $\mathcal{Q}_\eta = \{0 \leq v_l \leq \eta, l = 1, 2\}$ in P_2 and inside it the region S_η containing initial conditions that follow the connection $R_z \rightarrow \rho^2 PQ_w$ arriving at P_α at distance ε to the connection. Trajectories starting at S_η at a point $(u_1^0, \dots, u_4^0, v_1^0, v_2^0)$, with $(x, y) = (v_2^0, v_1^0)$, are mapped into P_α by the transition map $\psi(x, y) = (u_1, \dots, u_4, v_1, \alpha)$ given by:

$$u_l = u_l^0 \alpha^{v_l/\mu_2} x^{-v_l/\mu_2}, \quad l = 1, \dots, 4 \quad v_1 = \alpha^{\mu_1/\mu_2} y x^{-\mu_1/\mu_2}.$$

Recalling that the u_l^0 are constant in \mathcal{Q}_η it follows that S_η is mapped into a ruled surface in P_α generated by a curve $u_l = h_l(x)$, $l = 1, \dots, 4$ and containing lines through this curve and parallel to the v_1 axis.

We claim that $W^u(R_w)$ meets $W^s(\rho^2 PQ_w)$ transversely. From this, it follows that the v_1 axis is transverse to $W^s(\rho^2 PQ_w)$, since in these coordinates $W^u(R_w)$ is the plane $u_1 = 0$ and $W^s(\rho^2 PQ_w)$ contains the v_2 half-axis (the connection $R_z \rightarrow \rho^2 PQ_w$). Therefore the ruled surface $\psi(S_\eta)$ is transverse to the codimension 1 manifold $W^s(\rho^2 PQ_w)$.

To establish the claim, note that in the original coordinates the connection $R_z \rightarrow \rho^2 PQ_w$ takes place in the invariant plane

$$\tilde{V} = \text{Fix}(s_1, \gamma_\pi^1, r\gamma_{\pi/2}^1) = \{(x_1, 0, 0; 0, y, y), x, y \in \mathbf{R}\}$$

and this plane \tilde{V} is contained in the invariant subspace

$$V = \text{Fix}(\gamma_\pi^1, r\gamma_{\pi/2}^1) = \{(x_1, 0, 0; 0, y_2, y_3)\}$$

that also contains the nodes $\rho^2 R_w, \rho R_w, \rho^2 \widetilde{PQ}_w$ and their r -conjugates, as well as the corresponding connections. Moreover, $W^s(\rho^2 PQ_w) \cap V \subset \tilde{V}$, actually $W^s(\rho^2 PQ_w) \cap V$ consists of an open set in \tilde{V} containing the two connections $\pm R_z \rightarrow \rho^2 PQ_w$. The complementary direction to $W^s(\rho^2 PQ_w) \cap V$ in V is $W^u(\rho^2 PQ_w) \cap V = W^u(\rho^2 PQ_w)$, given by the connections $\rho^2 PQ_w \rightarrow \rho^2 R_w$ and $\rho^2 PQ_w \rightarrow \rho R_w$, so this direction is transverse to $W^s(\rho^2 PQ_w)$. Thus the two-dimensional $W^u(R_z) \subset V$ is transverse to $W^s(\rho^2 PQ_w)$, as claimed.

We have obtained a subset of a disk transverse to the $W_{loc}^s(R_z)$ that follows the connection $R_z \rightarrow \rho^2 PQ_w$. Any one-dimensional disk through $W_{loc}^s(R_z)$ contained in this subset will accumulate, after some time, in $W^u(\rho^2 PQ_w)$, by the λ -lemma. Now the arguments of the proof of the Krupa-Melbourne criterium (Theorem 2.7 in [13]) may be used without further adaptation to establish the stability of C_{12} . \square

A similar result holds for the cycle C_{23} but not for C_{34} . We had to exclude the cycle C_{34} from the hypothesis in order to obtain stability of C_{12} —it is not possible to get parameters where the 3 cycles exist and all other eigenvalues are negative.

7.4. Discussion. The stability results here are mainly for subnetwork Σ_{123} , which looks is like the one described by Kirk and Silber [12]. However, the dynamics is not the same. In this section we discuss this point. We start with the similarities.

Most of the motif for subnetwork Σ_{123} is contained in

$$\text{Fix}(\gamma_\pi^1) = \{(x, 0, 0, y_1, y_2, y_3) : x, y_1, y_2, y_3 \in \mathbf{R}\},$$

which we identify with \mathbf{R}^4 and where we have the symmetry group \mathbf{Z}_2^4 , as in the Kirk and Silber case, generated by the full symmetries in $\tilde{\Gamma}$:

$$\kappa_1 = \gamma_\pi^2 \quad \kappa_4 = s_1$$

and the hidden symmetries in Γ :

$$\kappa_2 = r\gamma_{\pi/2}^1 \quad \kappa_3 = s_1\gamma_{\pi/2}^3.$$

The first problem is that these symmetries do not work for the equations in \mathbf{R}^6 and if we change to \mathbf{C}^6 we start having 1- and 2-dimensional group orbits of connections.

The second problem is that this reduction has a lot more symmetries than the Kirk and Silber case. In particular,

$$\text{Fix}(\langle \rho, \rho^2, s_1, \gamma_\pi^1, \gamma_\pi^2 \rangle) = \{(0, 0, 0; y, y, y) \in \mathbf{R}^6\} \equiv \{(0, ; y, y, y) \in \mathbf{R}^4\}$$

is an invariant subspace (hexagons) that, together with some of its conjugates, prevents the connections $\rho^2 PQ_w \rightarrow R_w$ or $\rho^2 \widetilde{PQ}_w \rightarrow R_w$. So, we do not get connections $\rho^2 PQ_w \rightarrow R_w$ or $\rho^2 \widetilde{PQ}_w \rightarrow R_w$ inside this space, because hexagons are on the way.

The third problem is that since inside this subspace we do not get the connections that close the cycle, then we cannot do a direct application of the results of Kirk and Silber here. We could try to work on the quotient $\mathbf{R}^6/\tilde{\Gamma}$ but this is a complicated object, due to all the isotropy subgroups. More important, its regular part has dimension 6, so the global results obtained in 4 dimensions cannot be used.

The behaviour of trajectories near a railroad switch is in strong contrast to switching with complete freedom, as found in [2, 3]. The main difference is that here all eigenvalues are real, and this precludes global switching even with one transverse intersection of invariant manifolds.

Acknowledgements: The first two authors acknowledge support from Centro de Matemática da Universidade do Porto, financed by Fundação para a Ciência e a Tecnologia through the programmes POCTI and POSI.

REFERENCES

- [1] M.A.D. Aguiar and S.B.S.D. Castro. Chaotic and deterministic switching in a two-person game. *Working paper FEP* **305** (2008).
- [2] M.A.D. Aguiar, S.B.S.D. Castro and I.S. Labouriau. Dynamics near a heteroclinic network. *Nonlinearity* **18**, 391–414 (2005)
- [3] M.A.D. Aguiar, I.S. Labouriau and A.A.P. Rodrigues. Switching near a network. *Dynamical Systems* (to appear 2009)
- [4] D.V. Anosov, S.Kh. Aranson, V.I. Arnold, I.U. Bronshtein, V.Z. Grines, Yu.S. Il'yashenko. *Ordinary Differential Equations and Smooth Dynamical Systems*, Springer1988 *Dynamical Systems I, Vol. I of Encyclopædia of Mathematical Sciences*
- [5] E. Bodenschatz, W. Pesch and G. Ahlers Recent Developments in Rayleigh-Bénard Convection *Ann. Rev. Fluid Mech.* **32**, 709–778 (2000).
- [6] W. Brannath. Heteroclinic networks on the tetrahedron. *Nonlinearity* **7**, 1367–1384 (1994).
- [7] F.H. Busse and K.E. Heike. Convection in a rotating layer: a simple case of turbulence. *Science* **208**, 173–175 (1980).
- [8] B. Deng. The Sil'nikov problem, exponential expansion, strong λ -lemma, C^1 -linearization and homoclinic bifurcation. *J. Diff. Eq* **79**, 189–231 (1989).
- [9] A.V. Getling. *Rayleigh-Bénard convection: structures and dynamics*, World Scientific Publishing, (1998).
- [10] M. Golubitsky, I.N Stewart, and D. Schaeffer. *Singularities and Groups in Bifurcation Theory. Volume 2*. Appl. Math. Sci. **69**, Springer-Verlag, New York, (1988).
- [11] M. Golubitsky, J.W. Swift, and E. Knobloch. Symmetries and pattern selection in Rayleigh-Bénard convection, *Physica D*, **10**, 249–276 (1984).
- [12] V. Kirk and M. Silber. A competition between heteroclinic cycles. *Nonlinearity* **7**, 1605–1621 (1994).
- [13] M. Krupa and I. Melbourne. Asymptotic Stability of Heteroclinic Cycles in Systems with Symmetry. *Ergodic Theory and Dynam. Sys* **15**, 121–147 (1995).
- [14] M. Krupa and I. Melbourne. Asymptotic Stability of Heteroclinic Cycles in Systems with Symmetry II, *Proc. Roy. Soc. Edinburgh*, **134A**, 1177–1197 (2004).
- [15] G. Küppers and D. Lortz. Transition from laminar convection to thermal turbulence in a rotating fluid layer. *J. Fluid Mech.* **35**, 609–620 (1969).
- [16] I. Mercader, J. Prat and E. Knobloch. Robust heteroclinic cycles in two-dimensional Rayleigh-Bénard convection without Boussinesq symmetry. *Int. J. Bif. Chaos* **12**, 281–308 (2002).
- [17] J. Mizushima and K. Fujimura. Higher harmonic resonance of two-dimensional disturbances in Rayleigh-Bénard convection. *J. Fluid Mech.*, **234**, 651–667 (1992).
- [18] O. Podvigina. Stability of rolls in rotating magnetoconvection with physically realistic boundary conditions. preprint (2009).
- [19] O.M. Podvigina, and P.B. Ashwin. The $1 : \sqrt{2}$ mode interaction and heteroclinic networks in Boussinesq convection. *Physica D* **234**, 23–48 (2007).
- [20] J. Porter and E. Knobloch. Complex dynamics in the 1:3 spatial resonance. *Physica D* **143** 138–168 (2000).
- [21] J. Porter and E. Knobloch. New type of complex dynamics in the 1:2 spatial resonance. *Physica D* **159**, 125–154 (2001).
- [22] M.R.E. Proctor and C.A. Jones The interaction of two spatially resonant patterns in thermal convection. Part 1. Exact 1:2 resonance. *J. Fluid Mech.*, **188**, 301–355 (1988).
- [23] V.S. Samovol. Linearisation of systems of ordinary differential equations in a neighbourhood of invariant toroidal manifolds *Proc. Moscow Math. Soc.*, **38**, 187–219 (1979)

APPENDIX A. EIGENSPACES AND EIGENVALUES NEAR SINGLE-MODE STEADY STATES

Name	Subspace	Kernel (generators)	Action	Eigenvalues
R_z	$(q, 0, 0; 0, 0, 0)$	all	trivial	$2a_1x^2$
	$(iq, 0, 0; 0, 0, 0)$	$O(2) \times \mathbf{Z}_4 (\gamma^3, s_1; r\gamma_{\pi/2}^1)$	\mathbf{Z}_2	0
	$(0, u_2, u_3; 0, 0, 0)$	$\mathbf{Z}_3(\gamma_{2\pi/3}^3)$	$O(2) \times (\mathbf{Z}_4 \times \mathbf{Z}_2)$	$(a_2 - a_1)x^2$
	$(0, 0, 0; u, 0, 0)$	$\mathbf{D}_2 \times \mathbf{Z}_4 (s_2, \gamma_{\pi}^1; \gamma_{\pi/2}^3)$	$O(2) \times \mathbf{Z}_2$	$\lambda_2 + C_4x^2$
	$(0, 0, 0; 0, u, u)$	$\mathbf{D}_2 \times \mathbf{Z}_4 (s_2, \gamma_{\pi}^3; r\gamma_{\pi/2}^1)$	$O(2)$	$\lambda_2 + (C_5 + C_6)x^2$
	$(0, 0, 0; 0, u, -u)$	$\mathbf{Z}_2 \times \mathbf{Z}_4 (\gamma_{\pi/2}^3 s_2; r\gamma_{\pi/2}^1)$	$O(2) \times \mathbf{Z}_2$	$\lambda_2 + (C_5 - C_6)x^2$
PQ_z	$(q, 0, 0; 0, 0, 0)$	$\mathbf{D}_3 \times \mathbf{Z}_2 (s_1, \gamma_{2\pi/3}^3; s_2)$	\mathbf{D}_2	$(a_2 - a_1)x^2$
	$(iq, 0, 0; 0, 0, 0)$	$\mathbf{D}_3 \times \mathbf{Z}_2 (s_1, \gamma_{2\pi/3}^3; s_2 r\gamma_{\pi/3}^3)$	\mathbf{D}_2	$(a_2 - a_1)x^2$
	$(0, q, q; 0, 0, 0)$	all	trivial	$(a_1 + a_2)x^2$
	$(0, q, -q; 0, 0, 0)$	$\mathbf{D}_6 (s_3, r\gamma_{\pi/3}^3)$	\mathbf{Z}_2	$2(a_1 - a_2)x^2$
	$(0, iq, iq; 0, 0, 0)$	$\mathbf{D}_6 (s_1, r\gamma_{\pi/3}^3)$	\mathbf{Z}_2	0
	$(0, iq, -iq; 0, 0, 0)$	$\mathbf{D}_6 (s_2, r\gamma_{\pi/3}^3)$	\mathbf{Z}_2	0
	$(0, 0, 0; u_1, u_2, u_2)$	$\mathbf{Z}_2 (s_1)$	\mathbf{D}_6	$\mu_1 + \mu_2 = 2\lambda_2 + (C_4 + 3C_5)x^2$ $\mu_1\mu_2 = (\lambda_2 + 2C_5) \times$ $(\lambda_2 + (C_4 + 3C_5)x^2) - 2C_6x^2$
	$(0, 0, 0; 0, u_2, -u_2)$	$\mathbf{Z}_2 (s_1 r\gamma_{\pi}^3)$	$\mathbf{D}_3 \times \mathbf{Z}_2$	$2\lambda_2 + (C_4 + 3C_5)x^2$
	$(q, q, q; 0, 0, 0)$	all	trivial	$2(a_1 + a_2)x^2$
	$(iq, iq, iq; 0, 0, 0)$	$\mathbf{D}_3 \times \mathbf{Z}_3 (\rho^2, s_1; \gamma_{2\pi/3}^3)$	\mathbf{Z}_2	$-5a_3x^4$
$(q_1, q_2, q_3; 0, 0, 0),$ $q_1 + q_2 + q_3 = 0$	$\mathbf{D}_3 (s_3, \gamma_{2\pi/3}^3)$	\mathbf{D}_3	$2(a_1 - a_2)x^2$	
$(iq_1, iq_2, iq_3); 0, 0, 0)$ $q_1 + q_2 + q_3 = 0$	$\mathbf{Z}_3(\gamma_{2\pi/3}^3)$	\mathbf{D}_6	0	
$(0, 0, 0; u, u, u)$	$\mathbf{D}_3(\rho^2, s_2)$	\mathbf{D}_3	$\lambda_2 + (C_4 + 2C_5 + 2C_6)x^2$	
$(0, 0, 0; u_1, u_2, -(u_1 + u_2))$	empty	$\mathbf{D}_6 \times \mathbf{Z}_3$	$\lambda_2 + (C_4 + 2C_5 - C_6)x^2$	
T_z	$(iq, iq, iq; 0, 0, 0)$	all	trivial	$2(a_1 + a_2)x^2$
	$(q, q, q; 0, 0, 0)$	$\mathbf{D}_3 \times \mathbf{Z}_3 (\rho^2, s_1; \gamma_{2\pi/3}^3)$	\mathbf{Z}_2	$5a_3x^4$
	$(iq_1, iq_2, iq_3); 0, 0, 0),$ $q_1 + q_2 + q_3 = 0$	$\mathbf{D}_3 (rs_3, \gamma_{2\pi/3}^3)$	\mathbf{D}_3	$2(a_1 - a_2)x^2$
	$(q_1, q_2, q_3; 0, 0, 0),$ $q_1 + q_2 + q_3 = 0$	$\mathbf{Z}_3(\gamma_{2\pi/3}^3)$	\mathbf{D}_6	0
	$(0, 0, 0; u, u, u)$	$\mathbf{Z}_3(\rho^2)$	$\mathbf{D}_3 \times \mathbf{Z}_2$	$\lambda_2 + (C_4 + 2C_5 + 2C_6)x^2$
	$(0, 0, 0; u_1, u_2, -(u_1 + u_2))$	empty	$\mathbf{D}_6 \times \mathbf{Z}_3$	$\lambda_2 + (C_4 + 2C_5 - C_6)x^2$

TABLE 9. Eigenspaces and associated eigenvalues for (12) linearised near single-mode steady states for z modes.

Name	Subspace	Kernel (generators)	Action	Eigenvalues
R_w	(0, 0, 0; q, 0, 0)	all	trivial	$2B_1y^2$
	(0, 0, 0; iq, 0, 0)	$O(2) \times \mathbf{Z}_4 (\gamma^1, s_2; r\gamma_{\pi/4}^3)$	\mathbf{Z}_2	0
	(0, 0, 0; 0, u_2 , u_3)	$\mathbf{Z}_2 (\gamma_{\pi}^3)$	$O(2) \times \mathbf{D}_2$	$(B_2 - B_1)y^2$
	(u , 0, 0; 0, 0, 0)	$\mathbf{D}_2 \times \mathbf{Z}_4 (s_1, \gamma_{\pi}^1; \gamma_{\pi/2}^3)$	$O(2) \times \mathbf{Z}_2$	$\lambda_1 + C_1y^2$
	(0, u_2 , u_3 ; 0, 0, 0)	empty	$O(2) \times \mathbf{D}_4$	$\lambda_1 + C_2y^2$
PQ_w	(0, 0, 0; u , 0, 0)	$\mathbf{D}_2 (s_2, \gamma_{\pi}^1)$	\mathbf{D}_2	$(B_2 - B_1)y^2$
	(0, 0, 0; 0, q , q)	all	trivial	$(B_1 + B_2)y^2$
	(0, 0, 0; 0, q , $-q$)	$\mathbf{D}_4 (s_3, r\gamma_{\pi/2}^3)$	\mathbf{Z}_2	$(B_1 - B_2)y^2$
	(0, 0, 0; 0, iq , iq)	$\mathbf{D}_4 (s_1, r\gamma_{\pi/2}^3)$	\mathbf{Z}_2	0
	(0, 0, 0; 0, iq , $-iq$)	$\mathbf{D}_4 (s_2, r\gamma_{\pi/2}^3)$	\mathbf{Z}_2	0
	(q , 0, 0; 0, 0, 0)	$\mathbf{D}_2 \times \mathbf{Z}_4 (s_1, s_3; r\gamma_{\pi/2}^3)$	\mathbf{Z}_2	$\lambda_1 + (2C_2 + C_3)y^2$
	(iq , 0, 0; 0, 0, 0)	$\mathbf{D}_2 \times \mathbf{Z}_4 (s_1, r\gamma_{\pi/2}^1s_3; r\gamma_{\pi/2}^3s_3)$	\mathbf{Z}_2	$\lambda_1 + (2C_2 - C_3)y^2$
	(0, u_2 , u_3 ; 0, 0, 0)	empty	$\mathbf{D}_2 \times \mathbf{Z}_4$	$\lambda_1 + (C_1 + C_2)y^2$
H_w	(0, 0, 0; q , q , q)	all	trivial	$2(B_1 + B_2)y^2$
	(0, 0, 0; iq , iq , iq)	$\mathbf{D}_6 \times \mathbf{Z}_2 (\rho^2, s_1; \gamma_{\pi}^1)$	\mathbf{Z}_2	$-5B^3y^4$
	(0, 0, 0; q_1, q_2, q_3), $q_1 + q_2 + q_3 = 0$	$\mathbf{D}_2 (s_3, \gamma_{\pi}^1)$	\mathbf{D}_3	$2(B_1 - B_2)y^2$
	(0, 0, 0; iq_1, iq_2, iq_3), $q_1 + q_2 + q_3 = 0$	$\mathbf{Z}_2 (\gamma_{\pi}^1)$	\mathbf{D}_6	0
	(q_1, q_2, q_3 ; 0, 0, 0)	$\mathbf{Z}_2 (s_3)$	\mathbf{D}_6	$\lambda_1 + (C_1 + 2C_2 + C_3)y^2$
	(iq_1, iq_2, iq_3 ; 0, 0, 0)	empty	\mathbf{D}_6	$\lambda_1 + (C_1 + 2C_2 - C_3)y^2$
	(0, 0, 0; iq , iq , iq)	all	trivial	$2(B_1 + B_2)y^2$
T_w	(0, 0, 0; q , q , q)	$\mathbf{D}_3 \times \mathbf{Z}_2 (\rho^2, rs_1; \gamma_{\pi}^1)$	\mathbf{Z}_2	$-5B^3y^4$
	(0, 0, 0; iq_1, iq_2, iq_3), $q_1 + q_2 + q_3 = 0$	$\mathbf{D}_2 (rs_3, \gamma_{\pi}^1)$	\mathbf{D}_3	$2(B_1 - B_2)y^2$
	(0, 0, 0; q_1, q_2, q_3), $q_1 + q_2 + q_3 = 0$	$\mathbf{Z}_2 (\gamma_{\pi}^1)$	\mathbf{D}_6	0
	(iq_1, iq_2, iq_3 ; 0, 0, 0)	$\mathbf{Z}_2 (rs_3)$	\mathbf{D}_6	$\lambda_1 + (C_1 + 2C_2 + C_3)y^2$
	(q_1, q_2, q_3 ; 0, 0, 0)	empty	\mathbf{D}_6	$\lambda_1 + (C_1 + 2C_2 - C_3)y^2$

TABLE 10. Eigenspaces and associated eigenvalues for (12) linearised near single-mode steady states for w modes.